Cell Reports

Article

Emotional words evoke region- and valence-specific patterns of concurrent neuromodulator release in human thalamus and cortex

Graphical abstract

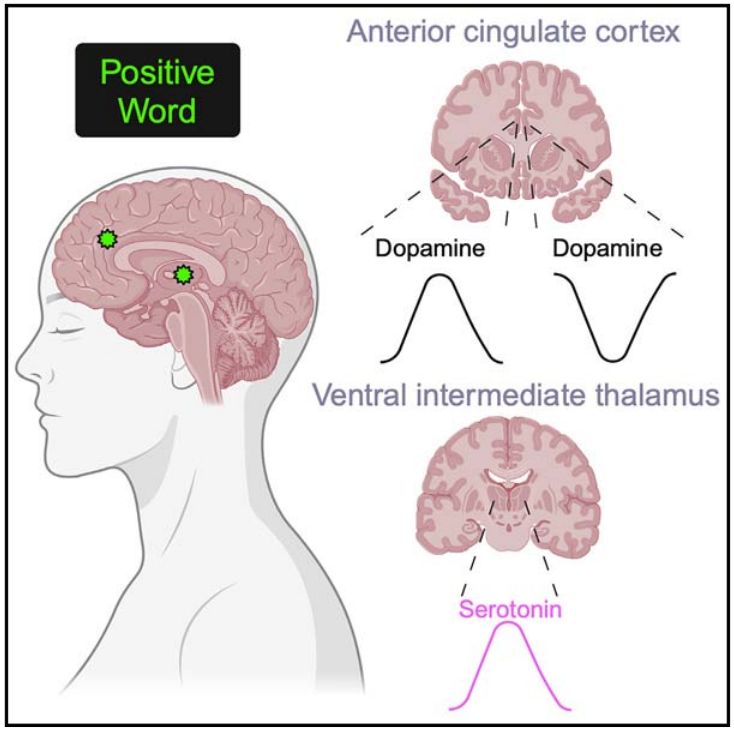

Authors

Seth R. Batten, Alec E. Hartle, Leonardo S. Barbosa, ..., Pearl Chiu, Pendleton R. Montague, William M. Howe

Correspondence

srbatten10@vtc.vt.edu (S.R.B.), read@vtc.vt.edu (P.R.M.), wmhowe@vt.edu (W.M.H.)

In brief

Batten et al. utilize a machine learning electrochemical approach to obtain a vector of monoamine neurotransmitters (dopamine, serotonin, and norepinephrine) in the thalamus and anterior cingulate cortex of conscious humans presented with affectively valenced words. Experiments reveal valence-specific signatures of monoamine release that were unique for thalamic and cortical recording sites.

Highlights

- Serotonin release is modulated by word valence in the thalamus
- Dopamine responses to valenced words vary between hemispheres in the anterior cingulate
- Norepinephrine is modulated by task demands and stimulus uncertainty in both brain areas
- Neuromodulator release patterns are regionally specific during language evaluation

Batten et al., 2025, Cell Reports *44*, 115162
January 28, 2025
https://doi.org/10.1016/j.celrep.2024.115162

CellPress

Cell Reports

CellPress
OPEN ACCESS

Article

Emotional words evoke region- and valence-specific patterns of concurrent neuromodulator release in human thalamus and cortex

Seth R. Batten,[1,14,16,*] Alec E. Hartle,[2,14] Leonardo S. Barbosa,[1,14] Beniamino Hadj-Amar,[3,14] Dan Bang,[1,4,5,6,14] Natalie Melville,[1] Tom Twomey,[1] Jason P. White,[1] Alexis Torres,[7] Xavier Celaya,[7] Samuel M. McClure,[7] Gene A. Brewer,[7] Terry Lohrenz,[1] Kenneth T. Kishida,[8,9] Robert W. Bina,[10] Mark R. Witcher,[1,11] Marina Vannucci,[3] Brooks Casas,[1,12] Pearl Chiu,[1,12] Pendleton R. Montague,[1,5,13,15,*] and William M. Howe[2,15,*]

[1]Fralin Biomedical Research Institute at VTC, Virginia Tech, Roanoke, VA 24016, USA
[2]School of Neuroscience, Virginia Tech, Blacksburg, VA 24060, USA
[3]Department of Statistics, Rice University, Houston, TX 77005, USA
[4]Center of Functionally Integrative Neuroscience, Aarhus University, 8000 Aarhus, Denmark
[5]Wellcome Centre for Human Neuroimaging, University College London, London WC1N 3BG, UK
[6]Department of Experimental Psychology, University of Oxford, Oxford OX2 6GG, UK
[7]Department of Psychology, Arizona State University, Tempe, AZ 85281, USA
[8]Department of Physiology and Pharmacology, Wake Forest School of Medicine, Winston-Salem, NC 27101, USA
[9]Department of Neurosurgery, Wake Forest School of Medicine, Winston-Salem, NC 27101, USA
[10]Department of Neurosurgery, Banner University Medical Center, Phoenix, AZ 85281, USA
[11]Division of Neurosurgery, Virginia Tech Carilion School of Medicine, Roanoke, VA 24014, USA
[12]Department of Psychology, Virginia Tech, Blacksburg, VA 24060, USA
[13]Department of Physics, Virginia Tech, Blacksburg, VA 24061, USA
[14]These authors contributed equally
[15]Senior author
[16]Lead contact
*Correspondence: srbatten10@vtc.vt.edu (S.R.B.), read@vtc.vt.edu (P.R.M.), wmhowe@vt.edu (W.M.H.)
https://doi.org/10.1016/j.celrep.2024.115162

SUMMARY

Words represent a uniquely human information channel—humans use words to express thoughts and feelings and to assign emotional valence to experience. Work from model organisms suggests that valence assignments are carried out in part by the neuromodulators dopamine, serotonin, and norepinephrine. Here, we ask whether valence signaling by these neuromodulators extends to word semantics in humans by measuring sub-second neuromodulator dynamics in the thalamus (N = 13) and anterior cingulate cortex (N = 6) of individuals evaluating positive, negative, and neutrally valenced words. Our combined results suggest that valenced words modulate neuromodulator release in both the thalamus and cortex, but with region- and valence-specific response patterns, as well as hemispheric dependence for dopamine release in the anterior cingulate. Overall, these experiments provide evidence that neuromodulator-dependent valence signaling extends to word semantics in humans, but not in a simple one-valence-per-transmitter fashion.

INTRODUCTION

The dopamine, serotonin, and norepinephrine systems—three of the brain's major neuromodulator systems—have all been implicated in valence-related neural computations.[1] Prevailing models suggest that dopamine release modulates both appetitive and aversive behaviors by encoding reward value, reward expectation, and stimulus salience.[2–9] Serotonin signaling appears necessary for both reward- and punishment-guided behavior,[10] may carry predictive value signals,[11] and has long been associated with cognitive control and emotion.[12] Neural activity in the norepinephrine producing neurons of the locus coeruleus has similarly been linked to the encoding of behavioral states, stimulus salience,[13–15] and effortful reward seeking[16] and may contribute to valence assignment through projections to limbic structures including the amygdala.[17] Importantly, accumulating evidence suggests that the relative balance of activity across these neuromodulator systems may be key for decision making,[18,19] and that normal control of behavior, cognition, and affect may depend upon these systems acting in concert.[20]

As critical as these findings are to understanding how the brain encodes valence, it is important to note that most of these studies have been conducted in model organisms. One central reason has been the lack of measurement techniques in humans that can parallel the highly spatiotemporally precise methods for studying neuromodulator dynamics in model organisms. As a

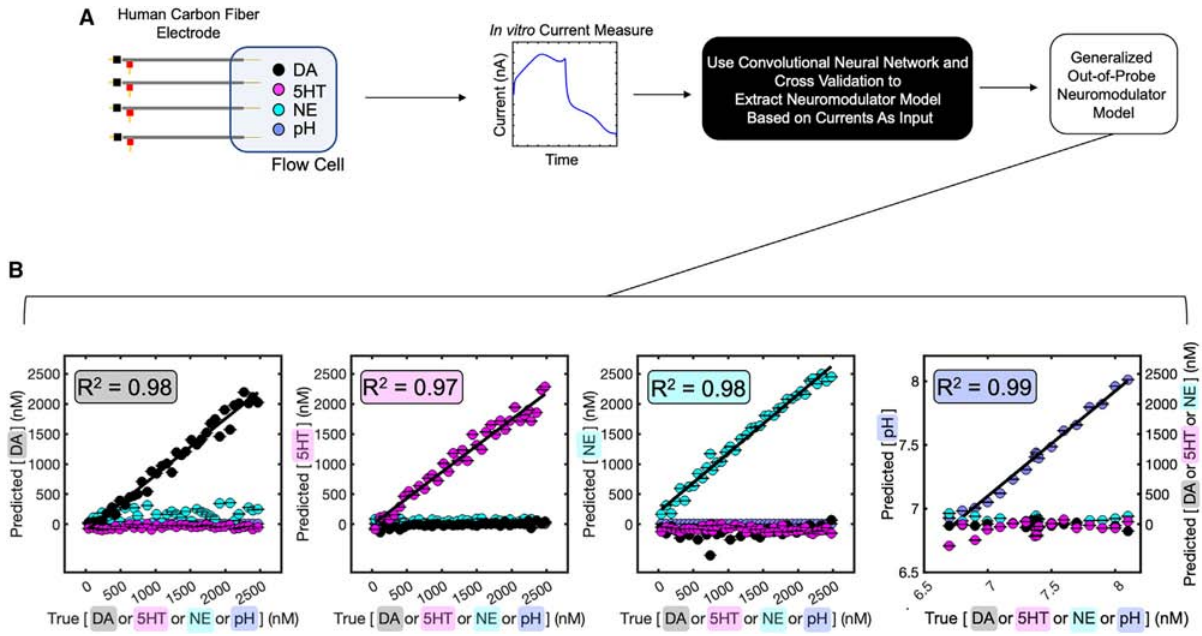

Figure 1. *In vitro* creation and validation of the carbon fiber electrode model

(A) The carbon fiber electrode model is created by first exposing carbon fiber electrodes to varying concentrations of dopamine (DA), serotonin (5HT), and norepinephrine (NE) against a background of varying pH under voltage clamp and measuring the currents for each analyte's concentration. These currents carry information about analyte identity and concentration. We then input these labeled data into a convolutional neural network (CNN), which generates a multi-analyte estimation model. We train this model using cross-validation and test it using out-of-electrode data. The model used here was trained on 70 electrodes.

(B) Results from the trained CNN model. Estimates (nM) for dopamine (DA; black; $R^2 = 0.98$), serotonin (5HT; magenta; $R^2 = 0.97$), norepinephrine (NE; cyan; $R^2 = 0.98$), and pH (lavender; $R^2 = 0.99$) are from out-of-sample concentrations from 6 held-out electrodes. The right y axis on the pH plot is showing that changes in pH are not confused for changes in neuromodulator concentration. Note that all predictions approximate y = x and error bars are barely visible at this scale. The black line represents the line of best fit. Data are represented as mean ± SEM across concentrations from different test electrodes.

result, our understanding of the underlying neurobiology of more abstract and uniquely human functions, such as the processing of valence-related word semantics, has fallen behind our growing understanding of basic cognitive functions that can be modeled in other species. This disparity represents a massive gap in our understanding of the neurobiology that underlies human subjective experience and defines human disease states.

Recently, significant progress has been made to bridge these gaps, by extending electrochemical techniques developed for use in model organisms to characterize sub-second neuromodulator fluctuations in the conscious human brain.[18,21–23] Convolutional neural networks originally crafted for time series classification[24] have been modified to optimize measurement selectivity for voltammetric data and enable the simultaneous characterization of moment-by-moment changes in dopamine, serotonin, and norepinephrine; these data can be obtained in task-performing humans in the context of deep brain stimulation (DBS) surgery or standard epilepsy monitoring.[18,19] Here, we deployed this approach to study how dopamine, serotonin, and norepinephrine may relate to the encoding of emotionally valenced words in the human brain. First, in people with essential tremor undergoing DBS surgery, we measured neuromodulator dynamics in the ventral intermediate nucleus of thalamus (VIM) during an emotional word task. Next, in epilepsy patients undergoing phase 2 monitoring, we measured neuromodulator dynamics in the anterior cingulate cortex (ACC), a structure known to be involved in the processing of emotional information[25,26] and language,[27] during the same affective word task.

RESULTS

Simultaneous monitoring of neuromodulator dynamics

We simultaneously measured dopamine, serotonin, and norepinephrine in the conscious human brain using (1) custom-made carbon fiber electrodes temporarily deployed during DBS surgery and (2) standard-of-care stereo-electroencephalography (sEEG) electrodes implanted for epilepsy monitoring. We first describe the electrochemical approach for carbon fiber electrodes, before later describing its extension to sEEG electrodes. The main difference is that carbon fiber electrodes allow for the training of a single model for neuromodulator estimation that can be applied across electrodes used for recording experiments, whereas the sEEG electrodes require the training of an individual estimation model for each electrode deployed.

Figure 1 details the workflow as well as the validation of the electrochemical approach for carbon fiber electrodes (see STAR Methods for full details). Briefly, a convolutional neural network model is trained on currents recorded *in vitro* using standard fast-scan cyclic voltammetry sweeps on electrodes

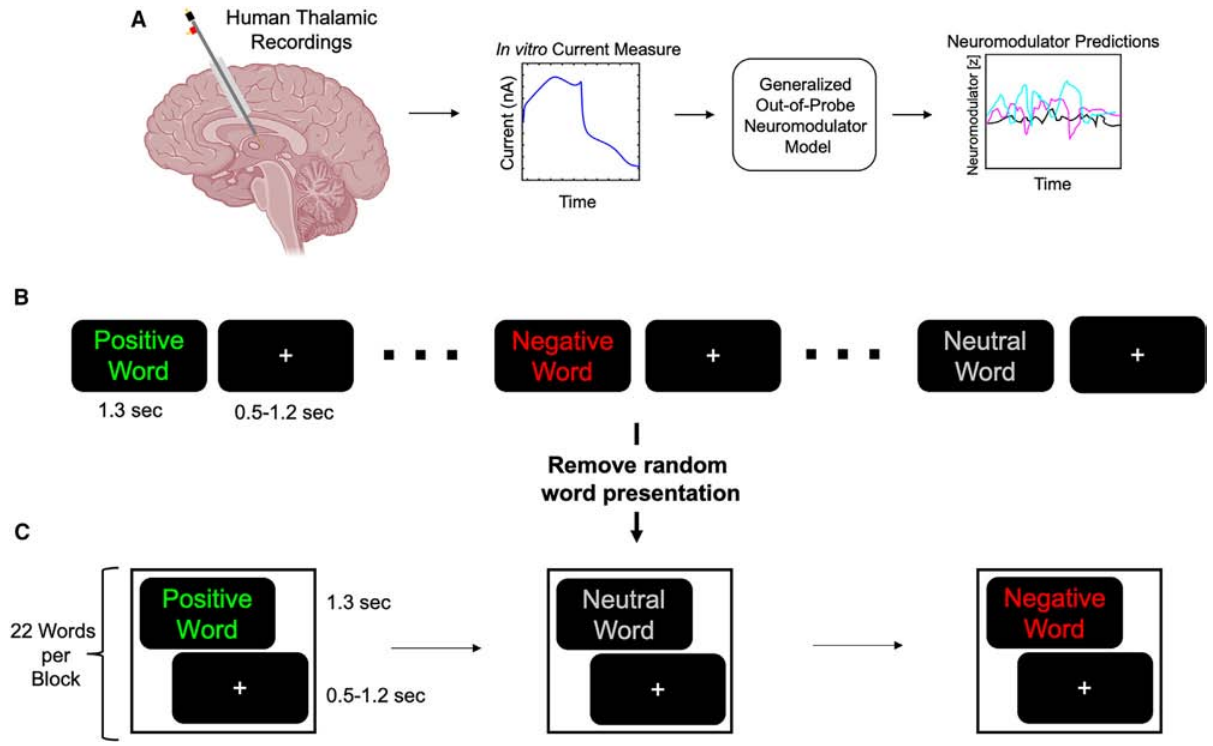

Figure 2. *In vivo* deployment of the carbon fiber electrode model during emotional word task

(A) The carbon fiber electrode model from Figure 1 was deployed in participants undergoing awake DBS surgery while they played an emotional word task. Currents were measured in the VIM of thalamus under voltage clamp and then entered into the estimation model to generate neuromodulator estimates.

(B) One group of participants ($n = 5$) played a randomized version of the emotional word task in which the positive, negative, and neutral words (trials) were shown in a random order. There were 44 negative words, 44 positive words, and 88 neutral words (176 trials in total). The participants' task was to label the color of the word.

(C) Another group of participants ($n = 9$) played a blocked version of the emotional word task where word valence was no longer randomized; instead, each block of 22 trials contained positive, negative, or neutral words. The words and participants' goal were the same as in the randomized version of the task.

exposed to known concentrations of dopamine, serotonin, and norepinephrine against a background of varying pH[18,19,22,23] (Figure 1A). The estimation model generalizes well to currents recorded from carbon fiber electrodes withheld from model training, and it does not confuse dopamine with either serotonin or norepinephrine and vice versa (Figure 1B; root mean square error $[RMSE]_{DA}$ = 106.87 nM; $RMSE_{5HT}$ = 121.61 nM; $RMSE_{NE}$ = 92.54 nM; $RMSE_{pH}$ = 0.038). In addition, in Figure S1, we demonstrate the *in vivo* sensitivity and specificity of the estimation model using optogenetics in mice (models 1–3 for statistical approach); for this demonstration, we selectively stimulated dopamine, serotonin, or norepinephrine cell bodies while measuring downstream neuromodulator release with the same carbon fiber electrode configuration used in the human DBS surgeries. It is worth noting that the carbon fiber model reported here is an updated model, based on additional training data compared to previously reported studies (e.g., Batten et al.[19]). This ability to continuously update and optimize our neurochemical inference strategy is specific to our approach. Further, this paper shows optogenetic validation of our model using the same human carbon fiber electrodes in rodents (Figure S1).

Neuromodulators selectively signal word arousal and valence in the thalamus

We applied the electrochemical approach for carbon fiber electrodes implanted in the VIM thalamus of participants ($n = 5$; see Table S1 for electrode coordinates) undergoing awake DBS surgery for the treatment of essential tremor (Figure 2A). Participants performed a variant of an emotional Stroop task,[28] here called the emotional word task.

Randomized emotional word task

On each trial, a word, written in one of 4 randomly assigned colors (red, blue, yellow, and green), was presented briefly (1.3 s), and the participant's task was to report the color of the word as quickly as possible using two button boxes placed in each hand (Figure 2B). The task was not self-paced; thus, the trials moved on whether participants were able to make a response or not. Only trials in which participants made a response were included in our analysis. Words were positively, negatively, or neutrally valenced drawn from the normed English language database, Affective Norms for Emotional Words (ANEW).[29] Positive and negative words differed significantly in ANEW valence ratings ($p < 0.05$ for all pairwise comparisons) but were matched

on ANEW arousal ratings (positive vs. negative words, $p > 0.1$; positive and negative vs. neutral words, both $p < 0.05$). The word valence categories were matched in terms of corpus frequency and word length. A task run consisted of 176 words (trials), separated by a fixation cross of variable duration (0.5–1.2 s). In this version of the task, word valence was randomized between trials.

Because individuals in DBS surgery cannot see their hands, and thus cannot see what buttons to push, button order was displayed on the screen. Using a trial-level linear mixed-effects model in which we predicted reaction times based on the continuous word valence and word arousal ANEW ratings (model 4), we found that participants' reaction times did not vary with either of the two variables (main effect of word valence, $F(1,775) = 0.30$, $p = 0.59$; main effect of word arousal, $F(1,775) = 0.43$, $p = 0.51$; Figure S2A). Thus, inclusion of the button order onscreen appeared to ease the cognitive load of the task and reduced the reaction time effect typically associated with affectively charged words in the standard emotional Stroop task.[28] Participants responded similarly across word valence categories (mean ± SEM; 91.8% ± 4.5% for negative words, 89.5% ± 6.0% for neutral words, and 91.4% ± 4.8% for positive words; Figure S2B), and they were overall highly accurate in their classification of word color (mean ± SEM; 0.91 ± 0.03 for negative words, 0.91 ± 0.01 for neutral words, and 0.91 ± 0.03 for positive words; Figure S2C).

Neuromodulator dynamics during valenced word presentation

We next turned to the measurements of neuromodulator dynamics in the VIM during word presentation. Specifically, for each trial, we computed the max change in each of the three neuromodulators during the 1.3-s window during which a word was shown relative to the average concentration in the 0.5 s prior to the onset of the word (see STAR Methods for discussion of this metric). We ran a separate trial-level linear mixed-effects model for each neuromodulator to test whether the max change values varied as a function of word valence, word arousal, reaction time, and their interactions. In this omnibus model, we used the continuous ANEW word valence and word arousal ratings as well as reaction time (given the recordings were from motor thalamus; model 5; see Figure S3A for neuromodulator time series). When main effects or interactions were observed in the omnibus models, we followed these up with separate mixed-effects models across valence categories or arousal states independently, to more directly probe the impact of these fixed effects. For consistency, reaction time and interaction terms were also included in these models.

The most robust effect detected with our omnibus tests was an effect of arousal scores on word-evoked changes in norepinephrine release. Specifically, the greatest change in norepinephrine release in VIM was observed in the presence of words with low arousal ratings (main effect of word arousal, $F(1,772) = 5.00$, $p = 0.03$; Figure 3A). Follow-up tests with arousal modeled as categorical variable supported this observation, with low arousal words being associated with greater VIM norepinephrine levels compared to high arousal words (model 6; $F(1,793) = 4.94$, $p = 0.03$). Although neither trend approached statistical significance (main effect of valence on serotonin and dopamine, $p > 0.05$), examination of the average max change estimates for dopamine and serotonin suggested that each was potentially modulated by the presentation of valanced words (Figure 3B; see Figure S3B for dopamine and serotonin responses to word arousal). Specifically, dopamine tended to decrease, whereas serotonin increased, when the word presented had a positive valence rating.

Blocked emotional word task

The absence of robust valence effects on dopamine and serotonin release was surprising in light of the vast literature implicating the two neuromodulators in valence-related neural computations.[1] Considering that norepinephrine varied as a function of word arousal in this randomly presented word task, a result that partially fits with its hypothesized role in tracking environmental uncertainty,[15] we reasoned that the lack of statistically robust changes in dopamine and serotonin could indicate that the unpredictable nature of word valence on a given trial masked valence-specific encoding by these systems. We therefore repeated the experiment in a larger cohort of participants ($n = 9$; see Table S1 for electrode coordinates) in a blocked version of the task. Here, 22 words of the same valence category were presented in succession, with blocks of neutral words interspersed between blocks of positive and negative words (Figure 2C); note that the task always began with a neutral block. For example, after the first neutral block, if the second block showed positive words, the next block would be neutral words, then negative words, then neutral words, etc. We reasoned that having blocks of words where the valence and time of word presentation were certain (except at the beginning of the block) might make neuromodulator fluctuations more strongly associated with affective identity. In other words, in the randomized version of the task, the valence of the next word is maximally uncertain (given the constraints of these designs), whereas in the blocked version the clear contrast might reveal valence-specific neuromodulator changes.

As for the randomized version, neither word valence nor arousal impacted reaction times in the blocked word valence task (model 4; main effect of word valence, $F(1,1413) = 0.31$, $p = 0.58$; main effect of word arousal, $F(1,1413) = 1.10$, $p = 0.29$; Figure S2D). Participants again responded similarly across word valence categories (mean ± SEM; 91.4% ± 3.76% for negative words, 90.0% ± 3.47% for neutral words, and 91.4% ± 2.69% for positive words; Figure S2E) and were overall highly accurate in their classification of word color (mean ± SEM; 0.76 ± 0.04 for negative words, 0.73 ± 0.04 for neutral words, and 0.73 ± 0.05 for positive words; Figure S2F).

Neuromodulator dynamics during valenced word presentation

We next ran separate trial-level linear mixed-effects analysis as described earlier to test whether our estimates of max change in dopamine, serotonin, and norepinephrine varied as a function of word valence, word arousal, reaction time, and their interactions (model 5). In support of the interpretation that the effect of word arousal on norepinephrine might be driven by valence uncertainty in the randomized task version, there was no effect of word arousal on norepinephrine in the blocked version (main effect of word arousal, $F(1,1410) = 1.16$, $p = 0.28$; Figure 3C). Norepinephrine also did not vary as a function of word valence

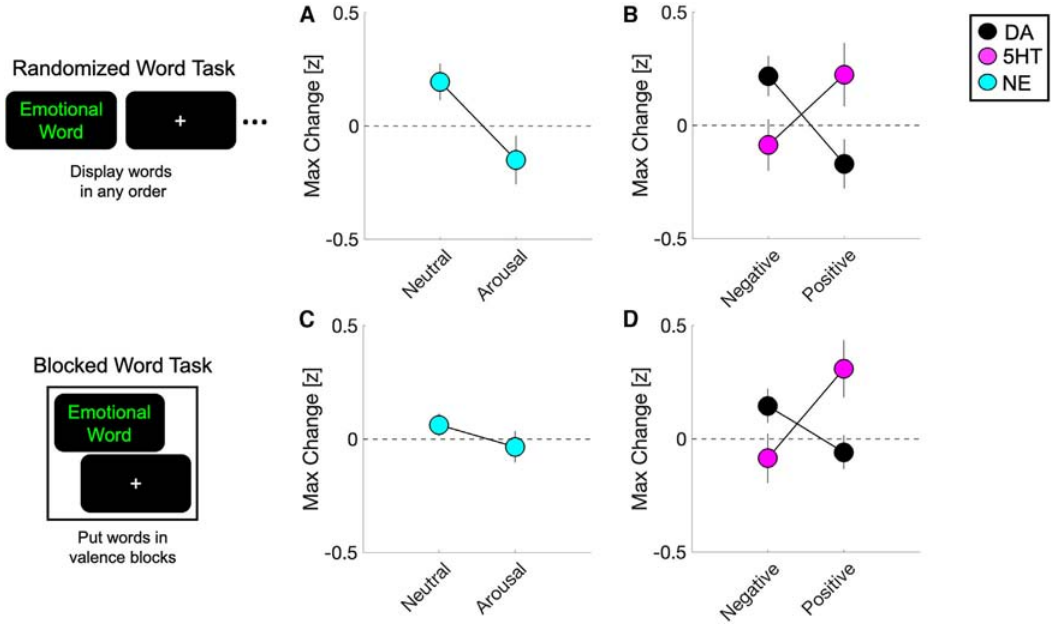

Figure 3. Neuromodulator dynamics in thalamus during randomized and blocked word task

(A) Norepinephrine (NE) significantly decreased as a function of word arousal during the random emotional word task (linear mixed-effects, $p < 0.05$).

(B) Dopamine (DA) decreased and serotonin (5HT) increased as a function of word valence during the random emotional word task, although this relationship did not reach statistical significance (linear mixed-effects, $p > 0.05$).

(C) Norepinephrine (NE) did not change as a function of word arousal during the blocked emotional word task where uncertainty about the word valence of the upcoming word was removed (linear mixed-effects, $p > 0.05$).

(D) Dopamine (DA) decreased as a function of word valence (although this did not reach significance, linear mixed-effects, $p > 0.05$) and serotonin (5HT) increased as a function of word valence (linear mixed-effects, $p < 0.05$) during the blocked emotional word task. Categorical linear mixed-effects models showed that serotonin had a greater response to positive words compared to negative words ($p < 0.05$) and that the response of serotonin for positive words was greater than that of dopamine to positive words ($p < 0.05$).

Data are presented as mean ± SEM across participants.

(main effect of word valence, $F(1,1410) = 1.48$, $p = 0.22$; Figure S3C). Turning to dopamine and serotonin, there were no effects of word arousal on the relative change in local concentrations of either neuromodulator (main effect of word arousal for dopamine, $F(1,1410) = 0.03$, $p = 0.87$; main effect of word arousal for serotonin, $F(1,1410) = 0.76$, $p = 0.38$; Figure S3D). Similar to the randomized version of the task, dopamine decreased as words became more positive, although, again, this effect of word valence did not reach significance (main effect of word valence, $F(1,1410) = 1.26$, $p = 0.26$; Figure 3D). Also, similar to the randomized version, serotonin increased as words became more positive; however, in this case this effect of word valence was statistically robust (main effect of word valence, $F(1,1410) = 4.72$, $p = 0.03$; Figure 3D). To further examine this relationship, we constructed a separate mixed-effects model focused on serotonin changes in response to positive and negatively valenced words. This analysis revealed that serotonin levels were greater in response to positive words compared to negative words (model 7; $F(1,720) = 4.94$, $p = 0.03$; Figure 3D). A separate model comparing changes in dopamine and serotonin release during positive word presentation supported that serotonin release was increased relative to dopamine when positive words were onscreen (model 8; $F(1,720) = 4.71$, $p = 0.03$; Figure 3D). This dissociation between serotonin and dopamine levels was not present in response to negative words (model 8; $F(1,720) = 1.76$, $p = 0.18$; Figure 3D).

Taken together, the results from the two cohorts indicate that neuromodulator release dynamics in the VIM are differentially modulated by the presentation of positive and negatively valenced words. However, this signal is clearly not robust at the level of the thalamus as rendered by this task. Interestingly, in the randomized version of the task, when the valence of the upcoming word was unpredictable, norepinephrine tracked the arousing qualities of words, independent of valence. In contrast, in the blocked version of the task, when the valence of the upcoming word was certain, norepinephrine encoding of word arousal was diminished. The most robust and statistically significant change observed with respect to valence was an increase in serotonin release in response to positive words.

Word valence and arousal modulate neuromodulator dynamics in the ACC

In the DBS setting, the recording sites are highly restricted by the clinical target, in this case the VIM of thalamus. The VIM would not typically be regarded as a critical structure for word or emotional processing; we nevertheless found interesting results

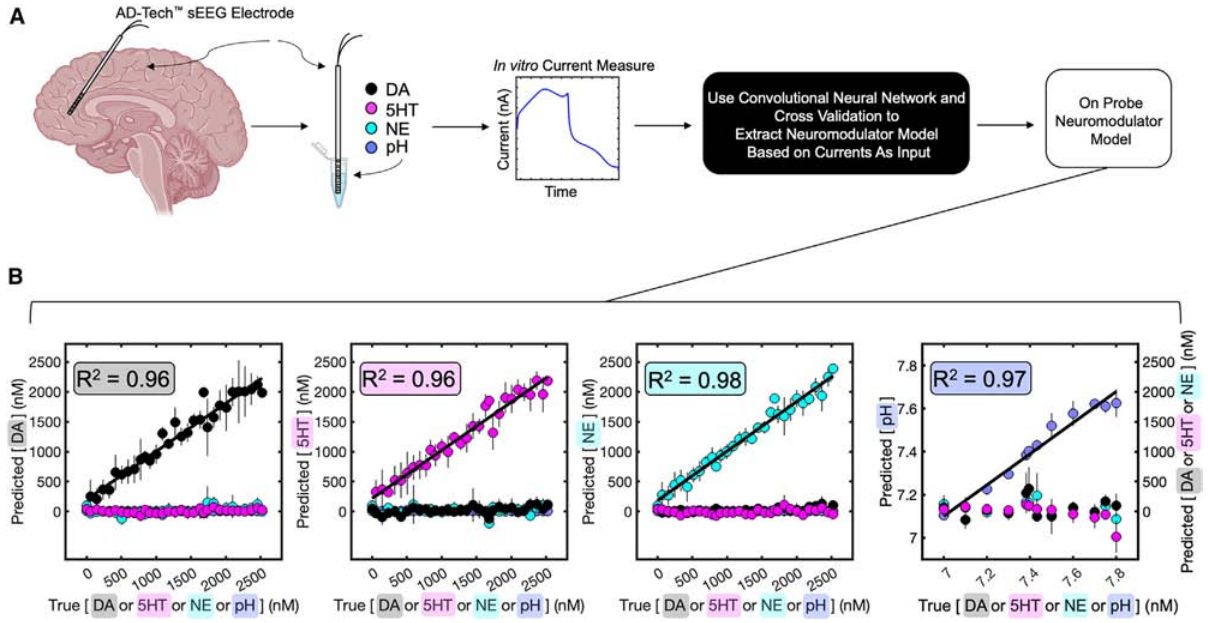

Figure 4. *In vitro* creation and validation of the sEEG electrode model

(A) Current measurements were taken from sEGG electrodes implanted in anterior cingulate cortex (ACC) while participants performed the blocked emotional word task shown in Figure 2C. Upon completion of the clinical protocol, the electrodes were explanted and given to the researchers. These electrodes were then exposed to varying concentrations of dopamine (DA), serotonin (5HT), and norepinephrine (NE) against a background of varying pH, and the resulting currents were measured. The currents, neuromodulator labels, and concentrations were used to train a convolutional neural network (CNN), which generates a multi-analyte estimation model similar to that in Figure 1B. The model was validated using data not included in the training set.

(B) Results from the trained CNN models. Estimates (nM) for dopamine (DA; black; $R^2 = 0.96$), serotonin (5HT; magenta; $R^2 = 0.96$), norepinephrine (NE; cyan; $R^2 = 0.98$), and pH (lavender; $R^2 = 0.97$) are from held-out concentrations from each electrode. The right y axis on the pH plot is showing that changes in pH are not confused for changes in neuromodulator concentration. Note that all predictions approximate y = x and error bars are barely visible for many points at this scale. The black line represents the line of best fit. Data are represented as mean ± SEM across concentrations from the different electrodes.

that suggest word valence effects on regional neuromodulator levels. However, given the evidence that different populations of projection neurons within the same neuromodulator system encode different information,[1,30–32] we wanted to test if the neuromodulator responses observed in the VIM are reflected in other brain areas, in particular ones that may be more directly involved in word and emotional processing.

As described in Bang et al. (2023),[33] the electrochemical approach for neuromodulator estimation using carbon fiber electrodes has recently been extended to clinical sEEG electrodes routinely used in phase 2 epilepsy monitoring (e.g., AD-Tech Behnke-Fried or Macro-Micro; see STAR Methods for details). This advance enables recordings from forebrain and cortical brain regions such as the ACC, a structure that has been directly linked to both language processing and affective control.[27,34–37] The basic logic of neuromodulator estimation is the same as for the carbon fiber electrodes used in the DBS setting. However, for sEEG electrodes, an individual estimation model is trained for the electrode used during *in vivo* data collection after being explanted by the neurosurgeon (Figure 4A). As shown in Figure 4B, the sEEG electrode models can detect and discriminate dopamine, serotonin, and norepinephrine against a background of varying pH. The sEEG electrode models generalize well to currents recorded from *in vitro* solutions not used for model training and does not confuse dopamine with either serotonin or norepinephrine and vice versa ($RMSE_{DA}$ = 136.00 nM; $RMSE_{5HT}$ = 125.21 nM; $RMSE_{NE}$ = 98.79 nM; $RMSE_{pH}$ = 0.034).

We applied the electrochemical approach for sEEG electrodes in the ACC of participants with epilepsy ($n = 6$; see Figure 5A for electrode placement) in the epilepsy monitoring unit (EMU). As we observed more specific valence effects in the blocked version of the task in our VIM cohort, EMU patients were only assessed with this version of the emotional word task (Figure 2C). As in the VIM cohorts, reaction times did not differ as a function of word valence (main effect of word valence, $F(1,1030) = 0.08$, $p = 0.78$; model 4; Figure S2G). However, there was a significant main effect of word arousal (main effect of arousal, $F(1,1030) = 5.06$, $p = 0.02$; Figure S4A), with slower responses for arousing words compared to neutral words. There are several possible reasons why an effect of word arousal on reaction times was seen in the context of epilepsy monitoring but not DBS surgery; for example, the potential interference properties of the task may have been stronger when performed outside the operating room in a more naturalistic setting and without any anesthesia. As in the VIM cohorts, participants responded similarly across word valence categories (mean ± SEM; 99.6% ± 0.35% for negative words, 99.8% ± 0.17% for neutral words, and 99.6% ± 0.35% for positive words; Figure S2H) and were highly accurate in their

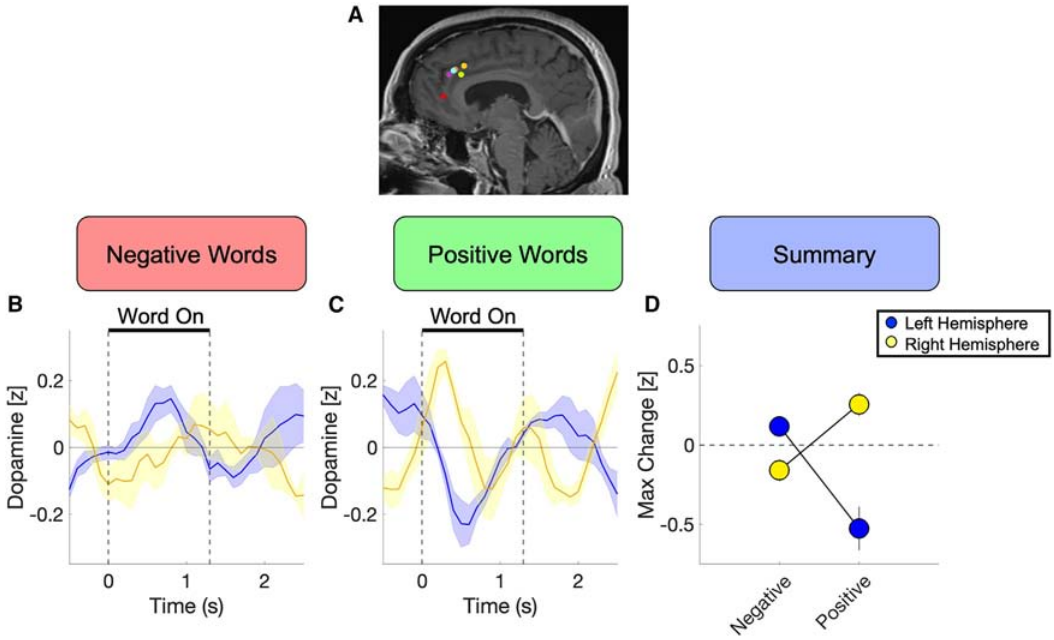

Figure 5. Dopamine changes to word valence are hemisphere dependent in the anterior cingulate cortex

(A) Representative brain image where each dot corresponds to a participant. Here, we display the dots on one hemisphere of a standard brain for simplicity even though the electrodes were implanted in different hemispheres. Note that the red dot is placed in a slightly different part of the ACC, due to its placement by a different neurosurgeon following a different clinical trajectory and using a slightly different model of sEEG electrode.

(B) Dopamine time series in the left (blue; $n = 3$) and right (yellow; $n = 3$) ACC around negative word presentation. Lines and shaded area represent mean ± SEM across participants per hemisphere.

(C) Dopamine time series in the left (blue) and right (yellow) ACC around positive word presentation. Lines and shaded area represent mean ± SEM across participants per hemisphere.

(D) Dopamine in the left ACC (blue) decreased as words became more positive (linear mixed-effects, $p < 0.05$). In the right ACC, dopamine changes followed the opposite pattern, increasing as words became more positive, although this did not reach significance (linear mixed-effects, $p > 0.05$). Across hemispheres, the dopamine response for positive words was greater in the right ACC compared to the left ACC (linear mixed-effects, $p < 0.05$). Data are represented as mean ± SEM across participants per hemisphere.

classification of word color (mean ± SEM; 0.99 ± 0.004 for negative words, 0.99 ± 0.003 for neutral words, and 1 ± 0 for positive words; Figure S2I).

Neuromodulator dynamics during valenced word presentation

For the analysis of the neurochemical data, we again focused on the estimates of max change in dopamine, serotonin, and norepinephrine during word presentation. In light of the vast literature supporting lateralization of language processing and affective control at the level of the cortex,[27,34–36,38–42] we added hemisphere to our models as a predictor along with all interactions in addition to word valence, word arousal, and reaction times (model 9). Similar to the VIM results from the blocked version of the task, we found that serotonin was modulated by word valence, though in the ACC this change was in interaction with reaction times (word valence × reaction time interaction, $F(1,1021) = 4.54$, $p = 0.03$). Specifically, serotonin increased as a function of reaction time when positive words were onscreen. In contrast, when negative words were presented, serotonin levels decreased as a function of reaction time (Figures S4C and S4D). We further probed this interaction using linear mixed-effects models with the effects of hemisphere and reaction time on serotonin changes during positive or negative valence words independently (model 10). These analysis suggests that the relationship between reaction time and valence was not particularly robust for serotonin, as the effect of reaction time on serotonin changes during negative words only reached the trend level ($F(1,259) = 3.55$, $p = 0.06$). In addition, we divided trials in to bins of fast and slow reaction times based on quartiles (see STAR Methods) and constructed linear mixed-effects models assessing serotonin changes on fast or slow reaction time trials, independently, as a function of valence and hemisphere (model 11). These tests also failed to identify robust differences in serotonin between valence categories within reaction time bins ($p > 0.05$). Notably, cerebral hemisphere had little impact on serotonin estimates in any of the models described earlier (e.g., from the omnibus model: word valence × hemisphere interaction, $F(1,1021) = 4.85 \times 10^{-6}$, $p = 1.00$; word valence × reaction time × hemisphere interaction, $F(1,1021) = 0.11$, $p = 0.74$). In contrast, analysis of dopamine estimates indicated that valence modulated word-evoked changes, but this was in interaction with hemisphere (word valence × hemisphere interaction, $F(1,1021) = 8.90$, $p = 0.003$). We further probed this interaction by looking at the effect of valence and reaction time

on dopamine levels within cerebral hemisphere (model 12). In the right hemisphere, graphically, dopamine increased in response to positive words relative to negative words; however, this trend did not reach significance ($F(1, 258) = 2.44$, $p = 0.12$; Figures 5B–5D). Word valence had a much more robust impact on dopamine changes within the left hemisphere and specifically was lower for positive words compared to negative words ($F(1, 260) = 7.65$, $p = 0.006$; Figures 5B–5D). Comparisons of dopamine changes to positive words across hemisphere (model 13) supported that dopamine levels were lower in the left hemisphere relative to the right hemisphere ($F(1, 259) = 9.51$, $p = 0.002$; Figure 5D). This hemispheric difference in word-evoked dopamine release was valence specific and not observed during negative words ($F(1, 259) = 1.35$, $p = 0.25$; Figure 5D). Somewhat surprisingly, given the patterns we observed in the thalamus during the blocked version of the word task, the omnibus analysis for norepinephrine in the ACC word arousal ratings appeared to impact changes in release in a hemisphere-dependent manner (Figure S4B). This pattern was a trend-level effect and did not reach statistical significance (arousal × hemisphere interaction ($F(1,1021) = 3.78$, $p = 0.05$). Graphically, and as shown Figure S4B, norepinephrine in the right ACC generally increased with word arousal, whereas norepinephrine in the left ACC—similar to the VIM results on the randomized version of the task—decreased with word arousal. Although this result did not pass our alpha threshold of 0.05, we conducted additional exploratory analyses comparing neutral and arousing words within hemisphere (model 14). These results suggested that the trend level interaction observed in the omnibus model was mostly driven by the right hemisphere ($F(1,521) = 3.12$, $p = 0.08$). Additionally, we compared responses to neutral and arousing words between hemispheres (model 15); this analysis revealed that, for neutral words, norepinephrine levels in the left and right hemisphere are only different at the trend level ($F(1,523) = 3.21$, $p = 0.07$) and there are no difference across hemispheres to arousing words ($F(1,522) = 1.42$, $p = 0.23$). Taken together, these nascent (i.e., $n = 3$ per hemisphere) results suggest that affective word presentation modulates neuromodulator release in the ACC. Serotonin in the ACC was modulated by word valence, although only in interaction with reaction times, and this relationship was not different between hemispheres. The most robust effects were observed for dopamine, where positive words were associated with lower dopamine release in the left hemisphere compared to negative words and where there was a significant difference across hemisphere for positive words. Indeed, no statistically significant effects of word valence were found when hemisphere was removed from the model (model 5; $p > 0.05$; Figure S4E).

Finally, given the impact of hemisphere on neuromodulator release in the ACC, we re-analyzed the VIM data including hemisphere as a predictor (same model used for ACC data, model 9). For the VIM cohort who performed the randomized task version (Figures S3E–S3H), there were no interactions between word valence and hemisphere for dopamine (word valence × hemisphere interaction, $F(1,766) = 0.58$, $p = 0.45$), serotonin (word valence × hemisphere interaction, $F(1,766) = 0.96$, $p = 0.33$), or norepinephrine (word valence × hemisphere interaction, $F(1,766) = 0.87$, $p = 0.35$). For the VIM cohort who performed the blocked task (Figures S3I–S3L), there were again no interactions between word valence and hemisphere for dopamine (word valence × hemisphere interaction, $F(1,1404) = 0.02$, $p = 0.88$), serotonin (word valence × hemisphere interaction, $F(1,1404) = 0.11$, $p = 0.74$), or norepinephrine (word valence × hemisphere interaction, $F(1,1404) = 1.77$, $p = 0.18$). Thus, lateralization of neuromodulator release in response to affective words was only observed at level of the ACC; see GitHub repository for tables of all statistical values.

DISCUSSION

Here, we measured sub-second dopamine, serotonin, and norepinephrine dynamics in the thalamus and in the ACC in conscious humans as they viewed emotionally evocative words of positive and negative valence, as well as neutral words (Figures 2B and 2C). The measurements from the thalamus—specifically the VIM—were obtained on carbon fiber electrodes deployed during awake DBS surgery for the treatment of essential tremor (Figures 1 and 2A), whereas the measurements from ACC were obtained on sEEG electrode implanted for epilepsy monitoring (Figure 4). While the role of VIM in higher-order processes is largely unknown, the ACC has long been implicated in the control of cognitive operations including language processing and affect.[27,34–37] Overall, the results support three general conclusions regarding the ascending monoamine systems: (1) word valence-related neuromodulator signals are regionally specific and detectable even at the level of motor structures like the VIM (Figure 3); (2) word valence-related neuromodulator signals are also detectable in the ACC, and, for dopamine, these valence signals are hemisphere dependent (Figure 5); and (3) norepinephrine release does not appear to be independently modulated by word valence in either the VIM (Figure 3; Figures S3A–S3C) or the ACC (Figure S4B).

That changes in dopamine levels, particularly in areas like ACC, may carry affective word-related information is broadly consistent with its long-hypothesized role in valence processing,[25,43–45] particularly in regard to positive affect.[46] However, dopamine responses, or the lack thereof, in the VIM are in contrast with many studies highlighting the role of dopamine in reward coding[47] (Figures 3B–3D). A growing body of literature supports a more nuanced role for dopamine in signaling valence and reward-related information; one where discrete populations of dopaminergic neurons are differentially engaged in the processing of different kinds of conditioned and unconditioned stimuli.[30–32] We believe our results are largely consistent with this emerging view. It is possible that the dopamine projections to the VIM are coming from a specialized subset of dopamine neurons that are not specifically tuned to stimulus valence, or not robustly modulated by abstract stimuli like language. Similarly, serotonin has been linked to punishment coding,[47] but also to signaling positive events depending on the timescale.[48] Here, we observed an increase in serotonin as words became more positive in the VIM (Figures 3B–3D), and a bi-directional relationship between serotonin and word valence based on response times at the level of the ACC.

The relationships between neuromodulator release dynamics and word valence reported here must be interpreted

conservatively. However, our observations agree with a model whereby each of the ascending monoamine projection networks shows a greater degree of topographic specificity in release than one might expect. Another potential inference from our work is that no neuromodulator signals valence alone but that valence is encoded by the relative change between them. For example, increases in dopamine with concurrent decreases in serotonin, and vice versa, may conjunctively encode stimulus valence. In fact, there is emerging evidence from studies in animal models for dopamine-serotonin interactions in valence processing.[49] Importantly, the approach we have developed and presented here provides the opportunity to explore this possibility in the brains of conscious humans.

In the ACC, we observed effects of word valence on dopamine that were hemisphere dependent. Specifically, dopamine increased in the right hemisphere as words became more positive and decreased in the left hemisphere (Figures 5B–5D). As described earlier, dopamine tracking both positive and negative events is in keeping with earlier studies,[30–32] as is the lateralization of valence processing. There are two prevailing lateralization theories about the processing of emotional content: (1) the right hemisphere hypothesis proposes that emotional processing is performed by the right hemisphere only, regardless of valence,[39] and (2) the valence-specific hypothesis proposes that different sides of the brain process different types of emotional content, namely that the right hemisphere processes negative emotions and the left hemisphere processes positive emotions.[42,50] There are also data that suggest that emotional valence processing is integrated across hemispheres.[41,51] One interpretation of our data is that, in ACC, dopamine may track word valence in a hemisphere-dependent fashion. However, it is important to keep in mind that our data would not necessarily be expected to correspond one-to-one with previous studies either directly or indirectly measuring neural activity. Our approach directly measures chemical neurotransmission, and the post-synaptic effect of neuromodulator release is dependent upon local signaling mechanisms. Furthermore, the strength of lateralized emotional signals during word processing reported in previous studies is highly state dependent,[52] so the directionality of predicted effects is not straightforward. One other possible interpretation is that divergent dopamine changes in the left and right hemisphere together may signal word valence as an integrated mechanism. The current work cannot adjudicate these interpretations, but these data do suggest that valence signaling and emotional processing are likely more nuanced than previously described. There is some evidence that the dopamine, serotonin, and norepinephrine systems are all lateralized.[53,54] In this light, it is interesting that we see lateralized effects of word valence for dopamine (Figures 5B–5D) but not serotonin (Figures S4C and S4D) release. More broadly, neuromodulator signaling may be specifically and simultaneously lateralized for some signals and not others, depending on the task at hand.

In this study, we also found some support for word arousal-related effects for norepinephrine in both the VIM and ACC. In the VIM, we only observed norepinephrine effects in the randomized version of the task, with norepinephrine decreasing as words became more arousing (Figure 3A). This result is unexpected given earlier evidence that increases in norepinephrine are generally associated with attention, vigilance, arousal, and gain control.[55,56] One potential reason could be that neutral words are more ambiguous than positive or negative words; when presented with several words that clearly fall into categories, the oddball words may be those that are ambiguous (neutral). In the ACC, we also observed that norepinephrine appeared more related to word arousal than valence, but in a hemisphere-dependent fashion (Figure S4B); norepinephrine increased in the right hemisphere as words became more arousing and decreased in the left hemisphere as words became more arousing. Data suggest that both norepinephrine signaling and arousal processing may also be lateralized,[40,41,53] which generally fits with our results. However, even here the largest difference in norepinephrine release between the hemispheres was observed when neutral words were onscreen, again, perhaps due to the oddball nature of neutral words in the current task. Regardless, these data suggest that both word valence and arousal dependent signals likely exist in the VIM and ACC and that this information might be carried by different neuromodulator systems.

The fact that we observed possible word valence and arousal effects in the VIM may seem surprising. However, the view of the thalamus as a simple "relay" between the environment and the cortex appears antiquated, as recent evidence shows that the thalamus is involved in arousal, cognition, conscious awareness, and even working memory.[57] Specifically, the VIM is traditionally considered to be a motor region of the thalamus,[58] with afferent connections from the cerebellum and brain stem and efferent connections to the pre- and post-central gyri.[59–61] Our results suggest that word valence processing may happen at the level of VIM—a finding one might not expect given the known motor involvement of this region. However, there is evidence that word processing does occur in circuits associated with motor function that are regular targets for movement disorders. For example, the caudate and other parts of the basal ganglia have been linked to suppressing irrelevant words at the level of action planning.[62] Further, there are differential electrophysiological signatures for the processing of negative versus neutral words in cortical areas associated with motor cortex.[63] Considering that the VIM has connections to both motor and sensory cortices,[59–61] it is not unreasonable to think that the VIM may also have a role in processing word semantics in a "motor planning" fashion. In fact, there is evidence from model organisms that motor thalamus[64] as well as other parts of thalamus[65] are critical for valence-like processing. Decoding the valence of a word almost certainly requires signals to be processed at the level of the cortex,[66,67] but considering VIM's cortex connections,[59–61] it may be a mediator in this process. The thalamus also has connections to the ACC,[68] which is involved in the processing of language and emotion.[26,69,70] Thus, it is not inconceivable that the neuromodulator signals measured in the VIM are somehow related to those we measured in the ACC.

It is worth further considering the potential origin of these neuromodulator signals in order to better contemplate their functional role. There is converging evidence that dopamine, serotonin, and norepinephrine are indeed present and detectable in the VIM.[71–74] The VIM receives serotonin innervation from the medial and dorsal raphe and dense norepinephrine innervation from the

locus coeruleus.[74–76] In the past, it was thought that the VIM did not receive much dopamine innervation; however, evidence now suggests that the VIM receives dopamine input from diverse sites such as hypothalamus, ventral mesencephalon, and lateral parabrachial nucleus.[77] Though it is intriguing that the VIM receives inputs from dopamine nuclei in regions that have been associated with both appetitive and aversive behavior (e.g., hypothalamus, lateral parabrachial nucleus), this diverse dopamine innervation admittedly makes interpretations about the function of dopamine release in the VIM more difficult. In contrast, it is well established that the ACC is innervated by the mesocortical dopamine system from the ventral tegmental area, the serotonin system from the raphe nucleus, and norepinephrine system from the locus coeruleus.[78–81] Thus, in the VIM, interpretations about the role and origin of these neuromodulators, especially dopamine, are more opaque. In contrast, interpretations about the origin of neuromodulator release in the ACC are more straightforward.

In sum, popular views of neurotransmission by ascending monoamine systems regard them as globally broadcasting valence and value signals throughout the brain,[82] and our collective data begin to support a model whereby word valence-related neuromodulator release may be tuned within discrete brain regions in humans. The presence of a possible word-valence signal by neuromodulator input to the thalamus and ACC means that other processing streams may have such evaluative signals available to modulate sensory information. More broadly, these data support the notion that the ancient systems that evolved to keep us alive by assessing positive and negative stimuli in the environment may extend to the processing of words—which are arguably equally critical to human survival. Our study lays the groundwork for understanding the dynamic orchestration of the neurochemical signaling that underlies uniquely human abilities and point to a potentially more nuanced picture of neuromodulator function revealed by these methods for simultaneous estimation.

Limitations of the study

The results presented here show changes in neuromodulator dynamics in response to the presentation of valenced words in conscious humans. Great care was taken to validate the methodology both *in vitro* and *in vivo*. Currently, there is no other methodology capable of producing these estimates in humans, and no other species that deploys symbolic language as means of communication as humans. Thus, there is very little in the way of previous work or parallel studies that can be used to benchmark our findings. Two limitations of this study stand out starkly. The first is the clinically imposed limitation of recording sites and the disease processes that determine them. It could very well be that the areas we have access to are not ideal for studying the way that neuromodulator systems encode word valence and thus our results underestimate the potency or consistency of signals that mediate language encoding. This point is particularly relevant for the recordings from the VIM thalamus, a structure that historically has been strongly linked to motor control. The second is the frank variability of the correlations between neuromodulators, word arousal, and word valence. For example, the apparent decline in norepinephrine at arousing word onset in the VIM is present in the randomized design and absent in the block design. One would expect that word valence surprise is removed in the block design and that word valence surprise is maximal in the random word presentation. However, in the ACC, arousal effects were more prevalent even in the block design. Thus, we do not see an easy rendering of these norepinephrine responses, and exactly what the norepinephrine fluctuations are encoding is therefore profoundly unclear. One possibility is that the downward nature of the fluctuation could have a differential impact on synapses onto inhibitory neurons versus excitatory neurons, but this study alone cannot resolve these perplexing findings. As neurochemical detection methods for use in humans continue to advance and proliferate, we acknowledge the interpretation of the computations supported by the signals detected and presented in our work will undoubtedly evolve.

RESOURCE AVAILABILITY

Lead contact

Requests for further information and resources should be directed to and will be fulfilled by the lead contact, Seth R. Batten (srbatten10@vtc.vt.edu).

Materials availability

This study did not generate new unique reagents.

Data and code availability

- De-identified human data have been deposited at GitHub as https://github.com/srbatten10/SR_Batten_et_al_Cell_Reports. They are publicly available as of the date of publication.
- All original code has been deposited at GitHub and is publicly available at https://github.com/srbatten10/SR_Batten_et_al_Cell_Reports as of the date of publication.
- Any additional information required to reanalyze the data reported in this paper is available from the lead contact upon request.

ACKNOWLEDGMENTS

We acknowledge Christopher Huck, Isaac Frank, Aidan Erwin, and Ronna Reed for their help with building carbon fiber electrodes and collecting data for neural network modeling. We acknowledge Cassie Efkeman, Duy Phan, Itamar Grunfeld, Isaac Levy, Brian Baker, and Rachel Silver for their help with the operational aspects of these experiments. We acknowledge Jacob Lee for coding the behavioral tasks. We acknowledge BioRender for cartoon electrodes (license number HE25Q0DWXR), mouse brain and gauge images in Figure S1 (license numbers CP270WMD6F, MJ270WN2PA, YY270WKIMM, HO27176SLF, TK27176UDL, VV27176WIV, CC27176YCR, and QR27176QTC), and human brain and Eppendorf (license numbers MQ25Q0EBI and WT27HX1Z9Q), which were created with BioRender.com. AAV-hSyn-hChR2(H134R)-EYFP was a gift from Karl Deisseroth (Addgene viral prep number 26973-AAV9; https://www.addgene.org/26973/). pAAV-EF1a-DIO-ChrimsonR-mRuby2-KV2.1-WPRE-SV40 was a gift from Christopher Harvey (Addgene viral prep number 124603-AAV9; http://n2t.net/addgene:124603).

We would also like to acknowledge our funding: Virginia Tech Foundation Seale Innovation Award (P.R.M.: FY22); Principal Research Fellowship funded by the Wellcome Trust (P.R.M.: 091188/Z/10/Z); Sir Henry Wellcome Postdoctoral Fellowship funded by the Wellcome Trust (D.B.: 213630/Z/18/Z); the Wellcome Centre for Human Neuroimaging, which is supported by core funding from the Wellcome Trust (D.B. and P.R.M.: 203147/Z/16/Z); the Lundbeck Foundation (D.B.: R368-2021-325); the Swartz Foundation (P.R.M.: 2019-11); the NIH NCATS (K.T.K.: KL2TR001421); the NIH-NIDA (K.T.K.: R01-DA048096); the NIH-NINDS (K.T.K. and P.R.M.: R01-NS092701); the NIH-NIMH (K.T.K.: R01-MH121099; K.T.K., M.V., and P.R.M.: R01-MH124115; P.C. and P.R.M.: R01-MH122512; B.C. and P.R.M.: R01-MH122948; and

P.C.: R01-127773); VA-RR&D (B.C.: D2354R); the NIH-NIA (W.M.H. and P.R.M.: R56 AG080735); and the Red Gates Foundation.

AUTHOR CONTRIBUTIONS

Conceptualization, P.C., P.R.M., B.C., W.M.H., S.R.B., T.L., and K.T.K.; data analysis, S.R.B., P.R.M., T.L., W.M.H., L.S.B., A.E.H., T.T., J.P.W., B.H.-A., D.B., and M.V.; data collection, M.R.W., R.W.B., S.R.B., N.M., A.E.H., A.T., and X.C.; funding acquisition, P.R.M., P.C., B.C., K.T.K., W.M.H., M.V., S.M.M., and G.A.B.; writing, P.R.M., S.R.B., T.L., D.B., L.S.B., W.M.H., A.E.H., B.H.-A., and M.V.

DECLARATION OF INTERESTS

The authors declare no competing interests.

STAR★METHODS

Detailed methods are provided in the online version of this paper and include the following:

- KEY RESOURCES TABLE
- EXPERIMENTAL MODEL AND STUDY PARTICIPANT DETAILS
  - Human participants
  - Rodent models
- METHOD DETAILS
  - Behavioral tasks
  - Human electrochemical approach
  - Rodent electrochemistry and optical stimulation
- QUANTIFICATION AND STATISTICAL ANALYSIS
  - Rodent neurochemical data analysis
  - Human behavioral data analysis
  - Human neurochemical data analysis

SUPPLEMENTAL INFORMATION

Supplemental information can be found online at https://doi.org/10.1016/j.celrep.2024.115162.

Received: July 31, 2024
Revised: November 4, 2024
Accepted: December 16, 2024
Published: January 7, 2025

REFERENCES

1. Tye, K.M. (2018). Neural Circuit Motifs in Valence Processing. Neuron *100*, 436–452. https://doi.org/10.1016/j.neuron.2018.10.001.
2. Robinson, T.E., and Berridge, K.C. (1993). The neural basis of drug craving: an incentive-sensitization theory of addiction. Brain Res. Brain Res. Rev. *18*, 247–291. https://doi.org/10.1016/0165-0173(93)90013-p.
3. Montague, P.R., Dayan, P., and Sejnowski, T.J. (1996). A framework for mesencephalic dopamine systems based on predictive Hebbian learning. J. Neurosci. *16*, 1936–1947. https://doi.org/10.1523/JNEUROSCI.16-05-01936.1996.
4. Wise, R.A. (2004). Dopamine, learning and motivation. Nat. Rev. Neurosci. *5*, 483–494. https://doi.org/10.1038/nrn1406.
5. Lemos, J.C., Wanat, M.J., Smith, J.S., Reyes, B.A.S., Hollon, N.G., Van Bockstaele, E.J., Chavkin, C., and Phillips, P.E.M. (2012). Severe stress switches CRF action in the nucleus accumbens from appetitive to aversive. Nature *490*, 402–406. https://doi.org/10.1038/nature11436.
6. Hamid, A.A., Pettibone, J.R., Mabrouk, O.S., Hetrick, V.L., Schmidt, R., Vander Weele, C.M., Kennedy, R.T., Aragona, B.J., and Berke, J.D. (2016). Mesolimbic dopamine signals the value of work. Nat. Neurosci. *19*, 117–126.
7. Saunders, B.T., Richard, J.M., Margolis, E.B., and Janak, P.H. (2018). Dopamine neurons create Pavlovian conditioned stimuli with circuit-defined motivational properties. Nat. Neurosci. *21*, 1072–1083. https://doi.org/10.1038/s41593-018-0191-4.
8. Mohebi, A., Pettibone, J.R., Hamid, A.A., Wong, J.-M.T., Vinson, L.T., Patriarchi, T., Tian, L., Kennedy, R.T., and Berke, J.D. (2019). Dissociable dopamine dynamics for learning and motivation. Nature *570*, 65–70. https://doi.org/10.1038/s41586-019-1235-y.
9. Kutlu, M.G., Zachry, J.E., Melugin, P.R., Cajigas, S.A., Chevee, M.F., Kelly, S.J., Kutlu, B., Tian, L., Siciliano, C.A., and Calipari, E.S. (2021). Dopamine release in the nucleus accumbens core signals perceived saliency. Curr. Biol. *31*, 4748–4761.e8. https://doi.org/10.1016/j.cub.2021.08.052.
10. Worbe, Y., Palminteri, S., Savulich, G., Daw, N.D., Fernandez-Egea, E., Robbins, T.W., and Voon, V. (2016). Valence-dependent influence of serotonin depletion on model-based choice strategy. Mol. Psychiatr. *21*, 624–629. https://doi.org/10.1038/mp.2015.46.
11. Harkin, E.F., Grossman, C.D., Cohen, J.Y., Béïque, J.-C., and Naud, R. (2023). Serotonin predictively encodes value. Preprint at bioRxiv. https://doi.org/10.1101/2023.09.19.558526.
12. Cools, R., Nakamura, K., and Daw, N.D. (2011). Serotonin and Dopamine: Unifying Affective, Activational, and Decision Functions. Neuropsychopharmacology *36*, 98–113. https://doi.org/10.1038/npp.2010.121.
13. Aston-Jones, G., Rajkowski, J., Kubiak, P., and Alexinsky, T. (1994). Locus coeruleus neurons in monkey are selectively activated by attended cues in a vigilance task. J. Neurosci. *14*, 4467–4480. https://doi.org/10.1523/JNEUROSCI.14-07-04467.1994.
14. Reimer, J., McGinley, M.J., Liu, Y., Rodenkirch, C., Wang, Q., McCormick, D.A., and Tolias, A.S. (2016). Pupil fluctuations track rapid changes in adrenergic and cholinergic activity in cortex. Nat. Commun. *7*, 13289. https://doi.org/10.1038/ncomms13289.
15. Yu, A.J., and Dayan, P. (2005). Uncertainty, neuromodulation, and attention. Neuron *46*, 681–692. https://doi.org/10.1016/j.neuron.2005.04.026.
16. Varazzani, C., San-Galli, A., Gilardeau, S., and Bouret, S. (2015). Noradrenaline and Dopamine Neurons in the Reward/Effort Trade-Off: A Direct Electrophysiological Comparison in Behaving Monkeys. J. Neurosci. *35*, 7866–7877. https://doi.org/10.1523/JNEUROSCI.0454-15.2015.
17. McCall, J.G., Siuda, E.R., Bhatti, D.L., Lawson, L.A., McElligott, Z.A., Stuber, G.D., and Bruchas, M.R. (2017). Locus coeruleus to basolateral amygdala noradrenergic projections promote anxiety-like behavior. Elife *6*, e18247. https://doi.org/10.7554/eLife.18247.
18. Bang, D., Kishida, K.T., Lohrenz, T., White, J.P., Laxton, A.W., Tatter, S.B., Fleming, S.M., and Montague, P.R. (2020). Sub-second Dopamine and Serotonin Signaling in Human Striatum during Perceptual Decision-Making. Neuron *108*, 999–1010.e6. https://doi.org/10.1016/j.neuron.2020.09.015.
19. Batten, S.R., Bang, D., Kopell, B.H., Davis, A.N., Heflin, M., Fu, Q., Perl, O., Ziafat, K., Hashemi, A., Saez, I., et al. (2024). Dopamine and serotonin in human substantia nigra track social context and value signals during economic exchange. Nat. Human Behav. *8*, 718–728. https://doi.org/10.1038/s41562-024-01831-w.
20. Briand, L.A., Gritton, H., Howe, W.M., Young, D.A., and Sarter, M. (2007). Modulators in concert for cognition: Modulator interactions in the prefrontal cortex. Prog. Neurobiol. *83*, 69–91. https://doi.org/10.1016/j.pneurobio.2007.06.007.
21. Kishida, K.T., Sandberg, S.G., Lohrenz, T., Comair, Y.G., Sáez, I., Phillips, P.E.M., and Montague, P.R. (2011). Sub-Second Dopamine Detection in Human Striatum. PLoS One *6*, e23291. https://doi.org/10.1371/journal.pone.0023291.
22. Kishida, K.T., Saez, I., Lohrenz, T., Witcher, M.R., Laxton, A.W., Tatter, S.B., White, J.P., Ellis, T.L., Phillips, P.E.M., and Montague, P.R. (2016). Subsecond dopamine fluctuations in human striatum encode superposed

error signals about actual and counterfactual reward. Proc. Natl. Acad. Sci. USA *113*, 200–205. https://doi.org/10.1073/pnas.1513619112.

23. Moran, R.J., Kishida, K.T., Lohrenz, T., Saez, I., Laxton, A.W., Witcher, M.R., Tatter, S.B., Ellis, T.L., Phillips, P.E., Dayan, P., and Montague, P.R. (2018). The Protective Action Encoding of Serotonin Transients in the Human Brain. Neuropsychopharmacology *43*, 1425–1435. https://doi.org/10.1038/npp.2017.304.
24. Ismail Fawaz, H., Lucas, B., Forestier, G., Pelletier, C., Schmidt, D.F., Weber, J., Webb, G.I., Idoumghar, L., Muller, P.-A., and Petitjean, F. (2020). Inceptiontime: Finding alexnet for time series classification. Data Min. Knowl. Discov. *34*, 1936–1962.
25. Bell, P.T., Gilat, M., Shine, J.M., McMahon, K.L., Lewis, S.J.G., and Copland, D.A. (2019). Neural correlates of emotional valence processing in Parkinson's disease: dysfunction in the subcortex. Brain Imaging Behav. *13*, 189–199. https://doi.org/10.1007/s11682-017-9754-3.
26. Kanske, P., and Kotz, S.A. (2011). Emotion Speeds up Conflict Resolution: A New Role for the Ventral Anterior Cingulate Cortex? Cerebr. Cortex *21*, 911–919. https://doi.org/10.1093/cercor/bhq157.
27. Binder, J.R., Frost, J.A., Hammeke, T.A., Cox, R.W., Rao, S.M., and Prieto, T. (1997). Human Brain Language Areas Identified by Functional Magnetic Resonance Imaging. J. Neurosci. *17*, 353–362. https://doi.org/10.1523/JNEUROSCI.17-01-00353.1997.
28. Ben-Haim, M.S., Williams, P., Howard, Z., Mama, Y., Eidels, A., and Algom, D. (2016). The emotional Stroop task: assessing cognitive performance under exposure to emotional content. JoVE J. Vis. Exp. *112*, e53720.
29. Bradley, M.M., and Lang, P.J. (1999). Affective norms for English words (ANEW): Instruction manual and affective ratings (Technical report C-1, the center for research in psychophysiology).
30. Matsumoto, M., and Hikosaka, O. (2009). Two types of dopamine neuron distinctly convey positive and negative motivational signals. Nature *459*, 837–841. https://doi.org/10.1038/nature08028.
31. Jo, Y.S., Heymann, G., and Zweifel, L.S. (2018). Dopamine Neurons Reflect the Uncertainty in Fear Generalization. Neuron *100*, 916–925.e3. https://doi.org/10.1016/j.neuron.2018.09.028.
32. Azcorra, M., Gaertner, Z., Davidson, C., He, Q., Kim, H., Nagappan, S., Hayes, C.K., Ramakrishnan, C., Fenno, L., Kim, Y.S., et al. (2023). Unique functional responses differentially map onto genetic subtypes of dopamine neurons. Nat. Neurosci. *26*, 1762–1774. https://doi.org/10.1038/s41593-023-01401-9.
33. Bang, D., Luo, Y., Barbosa, L.S., Batten, S.R., Hadj-Amar, B., Twomey, T., Melville, N., White, J.P., Torres, A., Celaya, X., et al. (2023). Noradrenaline tracks emotional modulation of attention in human amygdala. Curr. Biol. *33*, 5003–5010.e6. https://doi.org/10.1016/j.cub.2023.09.074.
34. Damasio, A.R., and Geschwind, N. (1984). The Neural Basis of Language. Annu. Rev. Neurosci. *7*, 127–147. https://doi.org/10.1146/annurev.ne.07.030184.001015.
35. Mayeux, R., and Kandel, E.R. (1985). Natural language, disorders of language, and other localizable disorders of cognitive function. In Principles of neural science (McGraw-Hill), pp. 688–703.
36. Lieberman, P. (2002). On the nature and evolution of the neural bases of human language. Am. J. Phys. Anthropol. *119*, 36–62. https://doi.org/10.1002/ajpa.10171.
37. Frömer, R., Lin, H., Dean Wolf, C.K., Inzlicht, M., and Shenhav, A. (2021). Expectations of reward and efficacy guide cognitive control allocation. Nat. Commun. *12*, 1030. https://doi.org/10.1038/s41467-021-21315-z.
38. Ahern, G.L., and Schwartz, G.E. (1979). Differential lateralization for positive versus negative emotion. Neuropsychologia *17*, 693–698. https://doi.org/10.1016/0028-3932(79)90045-9.
39. Borod, J.C., Cicero, B.A., Obler, L.K., Welkowitz, J., Erhan, H.M., Santschi, C., Grunwald, I.S., Agosti, R.M., and Whalen, J.R. (1998). Right hemisphere emotional perception: evidence across multiple channels. Neuropsychology *12*, 446–458.
40. Harrison, D.W. (2015). Right Hemisphere and Arousal. In Brain Asymmetry and Neural Systems: Foundations in Clinical Neuroscience and Neuropsychology, D.W. Harrison, ed. (Springer International Publishing), pp. 437–439. https://doi.org/10.1007/978-3-319-13069-9_25.
41. Zhang, J., Zhou, R., and Oei, T.P.S. (2011). The Effects of Valence and Arousal on Hemispheric Asymmetry of Emotion. J. Psychophysiol. *25*, 95–103. https://doi.org/10.1027/0269-8803/a000045.
42. Adolphs, R., Jansari, A., and Tranel, D. (2001). Hemispheric perception of emotional valence from facial expressions. Neuropsychology *15*, 516–524. https://doi.org/10.1037/0894-4105.15.4.516.
43. Fleury, V., Cousin, E., Czernecki, V., Schmitt, E., Lhommée, E., Poncet, A., Fraix, V., Troprès, I., Pollak, P., Krainik, A., and Krack, P. (2014). Dopaminergic modulation of emotional conflict in Parkinson's disease. Front. Aging Neurosci. *6*, 164. https://doi.org/10.3389/fnagi.2014.00164.
44. McIntosh, L.G., Mannava, S., Camalier, C.R., Folley, B.S., Albritton, A., Konrad, P.E., Charles, D., Park, S., and Neimat, J.S. (2014). Emotion recognition in early Parkinsonâ€™s disease patients undergoing deep brain stimulation or dopaminergic therapy: a comparison to healthy participants. Front. Aging Neurosci. *6*, 349. https://doi.org/10.3389/fnagi.2014.00349.
45. Martínez-Fernández, R., Kibleur, A., Chabardès, S., Fraix, V., Castrioto, A., Lhommée, E., Moro, E., Lescoules, L., Pelissier, P., David, O., et al. (2018). Different effects of levodopa and subthalamic stimulation on emotional conflict in Parkinson's disease. Hum. Brain Mapp. *39*, 5014–5027. https://doi.org/10.1002/hbm.24341.
46. Goschke, T., and Bolte, A. (2014). Emotional modulation of control dilemmas: The role of positive affect, reward, and dopamine in cognitive stability and flexibility. Neuropsychologia *62*, 403–423. https://doi.org/10.1016/j.neuropsychologia.2014.07.015.
47. Boureau, Y.-L., and Dayan, P. (2011). Opponency Revisited: Competition and Cooperation Between Dopamine and Serotonin. Neuropsychopharmacology *36*, 74–97. https://doi.org/10.1038/npp.2010.151.
48. Cohen, J.Y., Amoroso, M.W., and Uchida, N. (2015). Serotonergic neurons signal reward and punishment on multiple timescales. Elife *4*, e06346. https://doi.org/10.7554/eLife.06346.
49. Wert-Carvajal, C., Reneaux, M., Tchumatchenko, T., and Clopath, C. (2022). Dopamine and serotonin interplay for valence-based spatial learning. Cell Rep. *39*, 110645. https://doi.org/10.1016/j.celrep.2022.110645.
50. Ahern, G.L., and Schwartz, G.E. (1985). Differential lateralization for positive and negative emotion in the human brain: EEG spectral analysis. Neuropsychologia *23*, 745–755. https://doi.org/10.1016/0028-3932(85)90081-8.
51. Killgore, W.D.S., and Yurgelun-Todd, D.A. (2007). The right-hemisphere and valence hypotheses: could they both be right (and sometimes left)? Soc. Cognit. Affect Neurosci. *2*, 240–250. https://doi.org/10.1093/scan/nsm020.
52. Smith, S.D., and Bulman-Fleming, M.B. (2004). A hemispheric asymmetry for the unconscious perception of emotion. Brain Cogn. *55*, 452–457. https://doi.org/10.1016/j.bandc.2004.02.064.
53. Fitzgerald, P.J. (2012). Whose side are you on: Does serotonin preferentially activate the right hemisphere and norepinephrine the left? Med. Hypotheses *79*, 250–254. https://doi.org/10.1016/j.mehy.2012.05.001.
54. Molochnikov, I., and Cohen, D. (2014). Hemispheric differences in the mesostriatal dopaminergic system. Front. Syst. Neurosci. *8*, 110. https://doi.org/10.3389/fnsys.2014.00110.
55. Aston-Jones, G., and Cohen, J.D. (2005). AN INTEGRATIVE THEORY OF LOCUS COERULEUS-NOREPINEPHRINE FUNCTION: Adaptive Gain and Optimal Performance. Annu. Rev. Neurosci. *28*, 403–450. https://doi.org/10.1146/annurev.neuro.28.061604.135709.
56. Arnsten, A.F.T. (2009). The Emerging Neurobiology of Attention Deficit Hyperactivity Disorder: The Key Role of the Prefrontal Association Cortex. J. Pediatr. *154*, I–S43. https://doi.org/10.1016/j.jpeds.2009.01.018.

57. Shine, J.M., Lewis, L.D., Garrett, D.D., and Hwang, K. (2023). The impact of the human thalamus on brain-wide information processing. Nat. Rev. Neurosci. *24*, 416–430.

58. Helmich, R.C. (2018). The cerebral basis of Parkinsonian tremor: A network perspective. Mov. Disord. *33*, 219–231. https://doi.org/10.1002/mds.27224.

59. Benabid, A.L., Pollak, P., Gervason, C., Hoffmann, D., Gao, D.M., Hommel, M., Perret, J.E., and de Rougemont, J. (1991). Long-term suppression of tremor by chronic stimulation of the ventral intermediate thalamic nucleus. Lancet *337*, 403–406.

60. Zhang, J.-R., Feng, T., Hou, Y.-N., Chan, P., and Wu, T. (2016). Functional connectivity of vim nucleus in tremor-and akinetic-/rigid-dominant Parkinson's disease. CNS Neurosci. Ther. *22*, 378–386.

61. Tsolaki, E., Downes, A., Speier, W., Elias, W.J., and Pouratian, N. (2018). The potential value of probabilistic tractography-based for MR-guided focused ultrasound thalamotomy for essential tremor. Neuroimage. Clin. *17*, 1019–1027.

62. Ali, N., Green, D.W., Kherif, F., Devlin, J.T., and Price, C.J. (2010). The Role of the Left Head of Caudate in Suppressing Irrelevant Words. J. Cogn. Neurosci. *22*, 2369–2386. https://doi.org/10.1162/jocn.2009.21352.

63. Dissanayaka, N.N.W., Au, T.R., Angwin, A.J., O'Sullivan, J.D., Byrne, G.J., Silburn, P.A., Marsh, R., Mellick, G.D., and Copland, D.A. (2017). N400 and emotional word processing in Parkinson's disease. Neuropsychology *31*, 585–595. https://doi.org/10.1037/neu0000333.

64. Moll, F.W., Kranz, D., Corredera Asensio, A., Elmaleh, M., Ackert-Smith, L.A., and Long, M.A. (2023). Thalamus drives vocal onsets in the zebra finch courtship song. Nature *616*, 132–136. https://doi.org/10.1038/s41586-023-05818-x.

65. Li, H., Namburi, P., Olson, J.M., Borio, M., Lemieux, M.E., Beyeler, A., Calhoon, G.G., Hitora-Imamura, N., Coley, A.A., Libster, A., et al. (2022). Neurotensin orchestrates valence assignment in the amygdala. Nature *608*, 586–592. https://doi.org/10.1038/s41586-022-04964-y.

66. Moses, D.A., Metzger, S.L., Liu, J.R., Anumanchipalli, G.K., Makin, J.G., Sun, P.F., Chartier, J., Dougherty, M.E., Liu, P.M., Abrams, G.M., et al. (2021). Neuroprosthesis for decoding speech in a paralyzed person with anarthria. N. Engl. J. Med. *385*, 217–227.

67. Jamali, M., Grannan, B., Cai, J., Khanna, A.R., Muñoz, W., Caprara, I., Paulk, A.C., Cash, S.S., Fedorenko, E., and Williams, Z.M. (2024). Semantic encoding during language comprehension at single-cell resolution. Nature *631*, 610–616. https://doi.org/10.1038/s41586-024-07643-2.

68. Davis, K.D., Taub, E., Duffner, F., Lozano, A.M., Tasker, R.R., Houle, S., and Dostrovsky, J.O. (2000). Activation of the anterior cingulate cortex by thalamic stimulation in patients with chronic pain: a positron emission tomography study. Neurosurg. Focus *8*, 1–6. https://doi.org/10.3171/foc.2000.8.2.7.

69. Stevens, F.L., Hurley, R.A., and Taber, K.H. (2011). Anterior Cingulate Cortex: Unique Role in Cognition and Emotion. J. Neuroparasitol. *23*, 121–125. https://doi.org/10.1176/jnp.23.2.jnp121.

70. Citron, F.M.M. (2012). Neural correlates of written emotion word processing: A review of recent electrophysiological and hemodynamic neuroimaging studies. Brain Lang. *122*, 211–226. https://doi.org/10.1016/j.bandl.2011.12.007.

71. Meyerson, B.A., Linderoth, B., Karlsson, H., and Ungerstedt, U. (1990). Microdialysis in the human brain: Extracellular measurements in the thalamus of parkinsonian patients. Life Sci. *46*, 301–308. https://doi.org/10.1016/0024-3205(90)90037-R.

72. García-Cabezas, M.A., Martinez-Sanchez, P., Sanchez-Gonzalez, M.A., Garzon, M., and Cavada, C. (2009). Dopamine Innervation in the Thalamus: Monkey versus Rat. Cerebr. Cortex *19*, 424–434. https://doi.org/10.1093/cercor/bhn093.

73. Dirkx, M.F., Den Ouden, H.E.M., Aarts, E., Timmer, M.H.M., Bloem, B.R., Toni, I., and Helmich, R.C. (2017). Dopamine controls Parkinson's tremor by inhibiting the cerebellar thalamus. Brain *140*, 721–734. https://doi.org/10.1093/brain/aww331.

74. Kinnerup, M.B., Sommerauer, M., Damholdt, M.F., Schaldemose, J.L., Ismail, R., Terkelsen, A.J., Stær, K., Hansen, A., Fedorova, T.D., Knudsen, K., et al. (2021). Preserved noradrenergic function in Parkinson's disease patients with rest tremor. Neurobiol. Dis. *152*, 105295. https://doi.org/10.1016/j.nbd.2021.105295.

75. Caretti, V., Stoffers, D., Winogrodzka, A., Isaias, I.-U., Costantino, G., Pezzoli, G., Ferrarese, C., Antonini, A., Wolters, E.-C., and Booij, J. (2008). Loss of thalamic serotonin transporters in early drug-naïve Parkinson's disease patients is associated with tremor: an [123I]β-CIT SPECT study. J. Neural. Transm. *115*, 721–729. https://doi.org/10.1007/s00702-007-0015-2.

76. Isaias, I.U., Marzegan, A., Pezzoli, G., Marotta, G., Canesi, M., Biella, G.E.M., Volkmann, J., and Cavallari, P. (2011). A role for locus coeruleus in Parkinson tremor. Front. Hum. Neurosci. *5*, 179. https://doi.org/10.3389/fnhum.2011.00179.

77. Sánchez-González, M.A., García-Cabezas, M.A., Rico, B., and Cavada, C. (2005). The Primate Thalamus Is a Key Target for Brain Dopamine. J. Neurosci. *25*, 6076–6083. https://doi.org/10.1523/JNEUROSCI.0968-05.2005.

78. Berger, B., Trottier, S., Verney, C., Gaspar, P., and Alvarez, C. (1988). Regional and laminar distribution of the dopamine and serotonin innervation in the macaque cerebral cortex: A radioautographic study. J. Comp. Neurol. *273*, 99–119. https://doi.org/10.1002/cne.902730109.

79. Berger, B., Gaspar, P., and Verney, C. (1991). Dopaminergic innervation of the cerebral cortex: unexpected differences between rodents and primates. Trends Neurosci. *14*, 21–27. https://doi.org/10.1016/0166-2236(91)90179-X.

80. Schwarz, L.A., Miyamichi, K., Gao, X.J., Beier, K.T., Weissbourd, B., DeLoach, K.E., Ren, J., Ibanes, S., Malenka, R.C., Kremer, E.J., and Luo, L. (2015). Viral-genetic tracing of the input–output organization of a central noradrenaline circuit. Nature *524*, 88–92. https://doi.org/10.1038/nature14600.

81. Koga, K., Yamada, A., Song, Q., Li, X.-H., Chen, Q.-Y., Liu, R.-H., Ge, J., Zhan, C., Furue, H., Zhuo, M., and Chen, T. (2020). Ascending noradrenergic excitation from the locus coeruleus to the anterior cingulate cortex. Mol. Brain *13*, 49. https://doi.org/10.1186/s13041-020-00586-5.

82. Dayan, P. (2012). Twenty-Five Lessons from Computational Neuromodulation. Neuron *76*, 240–256. https://doi.org/10.1016/j.neuron.2012.09.027.

83. Abadi, M., Agarwal, A., Barham, P., Brevdo, E., Chen, Z., Citro, C., Corrado, G.S., Davis, A., Dean, J., Devin, M., et al. (2016). TensorFlow: Large-Scale Machine Learning on Heterogeneous Distributed Systems. Preprint at arXiv. https://doi.org/10.48550/arXiv.1603.04467.

84. Chollet, F. (2023). Keras resources.

85. Clark, J.J., Sandberg, S.G., Wanat, M.J., Gan, J.O., Horne, E.A., Hart, A.S., Akers, C.A., Parker, J.G., Willuhn, I., Martinez, V., et al. (2010). Chronic microsensors for longitudinal, subsecond dopamine detection in behaving animals. Nat. Methods *7*, 126–129. https://doi.org/10.1038/nmeth.1412.

86. Phillips, P.E.M., Stuber, G.D., Heien, M.L.A.V., Wightman, R.M., and Carelli, R.M. (2003). Subsecond dopamine release promotes cocaine seeking. Nature *422*, 614–618. https://doi.org/10.1038/nature01476.

87. He, K., Zhang, X., Ren, S., and Sun, J. (2016). Deep Residual Learning for Image Recognition (IEEE), pp. 770–778.

88. Kingma, D.P., and Ba, J. (2017). Adam: A Method for Stochastic Optimization. Preprint at arXiv. https://doi.org/10.48550/arXiv.1412.6980.

STAR★METHODS

KEY RESOURCES TABLE

REAGENT or RESOURCE	SOURCE	IDENTIFIER
Bacterial and virus strains		
AAV-hSyn-hChR2(H134R)-EYFP	Addgene (Karl Deisseroth);	RRID:Addgene_26973-AAV9
pAAV-EF1a-DIO-ChrimsonR-mRuby2-KV2.1-WPRE-SV40	Addgene (Christopher Harvey);	RRID:Addgene_124603-AAV9
Chemicals, peptides, and recombinant proteins		
Dopamine (DA)	Sigma-Aldrich	H8502; CAS: 62-31-7
Serotonin (5-HT)	Sigma-Aldrich	H9523; CAS: 153-98-0
Norepinephrine (NE)	Sigma-Aldrich	A7257; CAS: 51-41-2
Reagent for PBS: NaCl	Sigma-Aldrich	S7653-1K; CAS: 7647-14-5
Reagent for PBS: KCl	Sigma-Aldrich	P9333-1K; CAS: 447-40-7
Reagent for PBS: Na_2HPO	Sigma-Aldrich	S7907-1K; CAS: 7558-79-4
Reagent for PBS: KH_2HPO_4	Sigma-Aldrich	P5655-1K; CAS: 7778-77-0
Deposited data		
Human neural data, rodent neural data, human behavioral data	This paper	https://github.com/srbatten10/SR_Batten_et_al_Cell_Reports
Experimental models: Organisms/strains		
B6.SJL-*Slc6a3*$^{tm1.1(cre)Bkmn}$/J	Jackson Labs	RRID:IMSR_JAX:006660
B6.FVB(Cg)-Tg(Dbh-cre)KH212Gsat/Mmucd	MMRRC	RRID:MMRRC_036778-UCD
B6.129(Cg)-*Slc6a4*$^{tm1(cre)Xz}$/J	Jackson Labs	RRID:IMSR_JAX:014554
Software and algorithms		
pCLAMP	Molecular Devices	pCLAMP 10 Axon Instruments
MATLAB	MathWorks	MATLAB R2023b
Python	https://www.python.org	Python 3.9.7
R	https://www.r-project.org	R 4.2.0
Stan	https://mc-stan.org	Stan 2.21.0
TensorFlow	Abadi et al.[83]	TensorFlow 2.6.0
Keras	Chollet[84]	Keras 2.6.0
InceptionTime	Fawaz et al.[24]	https://arxiv.org/pdf/1909.04939
Code for reproducing figures	This paper	https://github.com/srbatten10/SR_Batten_et_al_Cell_Reports
Other		
470nm Fiber-Coupled LED	Thorlabs	M470F3
T-Cube LED Driver	Thorlabs	LEDD1B
635nm Red Diode Laser with Fiber Coupler (TA-FC)	Shanghai Laser & Optics Century Co.	RLM635TA-100FC
Headstage	Molecular Devices	CV-7B-EC Axon Instruments
Amplifier	Molecular Devices	Multiclamp 700B Axon Instruments
A/D Converter	Molecular Devices	Digidata 1550B Axon Instruments
Force function (TTL) generator	Tektronix	AFG320
Isolation transformer	Tripp Lite	IS500HG Isolation Transformer
Macro-micro electrode	Ad-Tech	MM16A-SP05X-000
Benhke-Fried electrode	Ad-Tech	BF08R-SP21X-0C2 (outer depth electrode) and WB09R-SP00X-0B6 (micro-wire bundle)
Carbon-fiber microelectrodes	Kishida et al.[22] Batten et al.[19]	In-house custom-made electrodes

EXPERIMENTAL MODEL AND STUDY PARTICIPANT DETAILS

Human participants

Five individuals with essential tremor (2 female, mean age ±SD = 72.8 ± 12.6 years) participated in the randomized word task experiment. Nine individuals with essential tremor (5 female, mean age ±SD = 71.3 ± 7.1 years) participated in the blocked word task experiment. Note one individual participated in both the blocked and randomized word task experiments with ~6 months in between because they came back for a second surgery. Six individuals with epilepsy (4 female, mean age ±SD = 34.2 ± 15 years) participated in the blocked word task experiment. Once the individuals with essential tremor had agreed to the DBS treatment, they were assessed for suitability for the research study and given the option to participate. Before obtaining informed written consent, the study and how it would alter the clinical procedure were explained– specifically, that the study would involve a research-exclusive electrode (carbon fiber electrode) and that extra time (maximum 30 min) would be needed to complete the study. The individuals with medication-resistant epilepsy were undergoing depth electrode implantation for phase II epilepsy monitoring. Prior to their stay in the epilepsy monitoring unit, the study was discussed with the participants and the clinical team. The study protocol was described verbally and participants provided both verbal and informed written consent. The study was approved by the IRB committee at Carilion Clinic (20–854 and 19–365), VT IRB (11–078), and Banner University Hospital IRB (STUDY00000295). No adverse or unanticipated events occurred during or as a result of the study. See Table S2 specific participant information. Note DBS patients were not on their daily medications during the experiment. However, epilepsy participants 14–18 were on their daily medications during the experiment.

Rodent models

DAT-Cre mice (Figures S1C–S1F, $N = 7$: 2 male, mean age ± SD = 160.4 ± 41.8 days; Figures S1H–S1K, $n = 4$: 4 female, mean age ± SD = 130 ± 12 days, a subset of mice used in Figures S1C–S1F), DBH-Cre mice (Figures S1M–S1P, $N = 3$: 3 male, mean age ± SD = 178.7 ± 11.8 days), and SERT-Cre mice (Figures S1R–S1U, $N = 3$: 2 male, mean age ± SD = 272.3 ± 56.1 days) were used for optogenetic experiments. DAT-Cre and DBH-Cre mice were injected with an AAV to drive Cre-recombinase-dependent expression of channelrhodopsin (ChR2, AAV-DIO-hChR2(H134R)-EYFP, Addgene viral prep # 26973-AAV9) in midbrain dopamine neurons and locus coeruleus neurons, respectively. SERT-Cre mice were injected with an AAV to drive Cre-recombinase-dependent expression of ChrimsonR (AAV-EF1a-DIO-ChrimsonR-mRuby2-KV2.1-WPRE-SV40, Addgene viral prep # 124603-AAV9) in serotonergic dorsal raphe nucleus. After viral injections and optic fiber surgeries (see below for details) all animals were housed separately. All mouse experiments were conducted in accordance with the ethical guidelines of the National Institutes of Health, and were approved by the Institutional Animal Care and Use Committee at Virginia Tech, Blacksburg, VA (protocol #23–112).

METHOD DETAILS

Behavioral tasks

On each trial, a word, written in one of 4 colors (red, blue, yellow, and green), was presented briefly (1.3 s), and the participants' task was to report the color of the word as quickly as possible using two button boxes placed in each hand. Critically, the words were positively, negatively, or neutrally valenced words– drawn from the normed English language database, Affective Norms for Emotional Words (ANEW),[29] and presented in either a randomized order (Figure 2B) or a block structure (Figure 2C). Positive and negative words differed significantly in ANEW valence ratings ($p < 0.05$ for all pairwise comparisons) but were matched on ANEW arousal ratings (positive vs. negative words, $p > 0.1$; positive and negative vs. neutral words, both $p < 0.05$). The word valence categories were matched in terms of corpus frequency and word length. A task run consisted of 176 words (trials), separated by a fixation cross of variable duration (0.5–1.2 s). Before the task began, participants had 50 trials practicing color matching where the words: "red", "blue", "yellow", or "green" (colored congruently) were shown on the screen and the task for the patient was to simply push the button corresponding to the color the word indicated. Because individuals in DBS surgery cannot see their hands, and thus cannot see what buttons to push, button order was displayed on the screen. For consistency, the epilepsy participants also had the button order displayed on the screen. Note that both version of the task (randomized, blocked) were not self-paced and were on regular time boundaries. Thus, the time-on-task was held constant across all participants.

Human electrochemical approach

In vivo *data acquisition for DBS participants*

We obtained voltammetry data in individuals undergoing DBS using carbon fiber microelectrodes constructed as described in Kishida et al., 2016.[22] Some participants' recordings were made using carbon-fiber microelectrodes slightly modified from those in Kishida et al., 2016.[22] For these electrodes Alpha Omega NeuroProbe Sonus guide tubes (STR-009080-10) were used as well as a longer (24.5 cm) and larger diameter (440 μm) glass capillary (Molex #1068450450). This change was made in order to accommodate new neurosurgical equipment. The voltammetry protocol was based on previous work in humans[18,19,21–23] and rodents.[85,86] The voltage forcing function used was a standard triangular voltage shape repeated at 10 Hz (ramp up from −0.6 V to +1.4 V at 400 V/s, and ramp down from +1.4 V to −0.6 V at 400 V/s [10ms] then hold at −0.6 V for 90 ms). The current response was recorded at a sampling rate of 100 kHz. We also used a 97Hz pre-cycle protocol prior to data collection to aid in microelectrode equilibration (i.e., allow the current to reach a baseline state). This pre-cycle protocol used the previously mentioned triangular voltage ramp repeated with a shorter

holding period (in order to accommodate the higher frequency triangular voltage ramp). The voltammetry recordings were made using Molecular Devices (Molecular Devices, LLC, San Jose, CA, 95134) equipment: the Axon Instruments MultiClamp 700B Patch Clamp Amplifier, the Electrochemistry Headstage (CV 7B-EC; slightly modified to allow larger current measures), and the Digidata 1550B Data Acquisition System.

In vivo *data acquisition for epilepsy participants*

We conducted fast-scan cyclic voltammetry (FSCV) on standard Ad-Tech Behnke-Fried (WB09R-SP00X-0B6) and macro-micro electrodes (MM16A-SP05X-000). The electrodes were stereotactically implanted to/explanted from the ACC. We used the wire bundle for the Behnke-Fried electrodes, using wire 9 as a reference electrode and any of the other 8 wires as working electrodes. For macro-micro electrodes, we used a longitudinally adjacent pair of micro-contacts on the electrode as our working and reference electrodes. Our FSCV protocol for Behnke-Fried electrodes was a modification on what we have previously used on depth electrodes in humans (Bang et al., 2023). Our measurement waveform was a standard triangular voltage ramp applied at 10 Hz (hold at −0.6 V for 90 ms, ramp up from −0.6 V to +0.175 V at 155 V/s, ramp down from +0.175 V to −0.6 V at −155 V/s). For macro-micro electrodes, we used the same protocol as previously reported (Bang et al., 2023) using a standard triangular voltage ramp applied at 10 Hz (hold at −0.6 V for 90 ms, ramp up from −0.6 V to +0.6 V at 240 V/s, ramp down from +0.6 V to −0.6 V at −240 V/s). We recorded the current response at 100 kHz. For *in vivo* experiments, we collected data for 1–2 min before starting the task to allow the electrode to equilibrate.

The voltammetry recordings were made using Molecular Devices (Molecular Devices, LLC, San Jose, CA, 95134) equipment: the Axon Instruments MultiClamp 700B Patch Clamp Amplifier, the Electrochemistry Headstage (CV 7B-EC; slightly modified to allow larger current measures), and the Digidata 1550B Data Acquisition System.

In vivo *neuromodulator estimates*

We estimated *in vivo* neuromodulator concentrations from *in vivo* current traces using an ensemble of deep convolutional neural networks that were trained and tested on *in vitro* data. The *in vitro* data consisted of voltammetry current traces obtained from multiple carbon fiber electrodes (for DBS participants) or explanted Ad-Tech depth electrodes (for epilepsy participants) exposed to known concentrations of dopamine, serotonin, norepinephrine, and pH. We modified the InceptionTime time series classification model[24] to perform multi-variate regression. The model was coded in Python using TensorFlow[83] and Keras.[84] We used equally weighted averages of *in vivo* concentration estimates from multiple InceptionTime models as in Fawaz et al., 2020.[24]

Specifically, the modified InceptionTime network is based on two ResNet[87] blocks. Each block contains 3 convolutional blocks while each convolutional block is composed of 4 convolutional layers in parallel, each with 32 filters and with increasing kernel sizes (1, 10, 20 and 40). The output of each of these convolutional layers is stacked together, after which batch normalization and RELU activations are applied. This output passes through a bottleneck convolutional layer with kernel size one and 32 filters and whose output serves as the input for the next convolutional block. To start the implementation of the ResNet architecture the input, after passing through another bottleneck convolutional layer with kernel size 1 and 32 filters, is added to the output of the first ResNet block, and, after activation, this serves as the input to the next ResNet block. The operation is repeated for the second ResNet block, except that the input is replaced by the output of the first ResNet block. Finally, after passing through a global average pooling, the output of the second ResNet block passes through a dense layer with four output nodes, which gives the predictions of the four analytes. All activation functions are RELU, except after the last dense layer, which uses softplus for the epilepsy electrode models and linear for the DBS electrodes models.

All models used the mean squared error loss. Training schedule used the ADAM optimizer,[88] with an initial learning rate of 1e-3 that halved after 5 epochs without decrease of validation loss. Carbon fiber electrode models did not have a minimum learning rate, while depth electrode models had a minimum learning rate of 1e-6. The batch size was 64. The loss on the validation set was calculated after each epoch. The model from the epoch with the lowest validation loss was selected as the final model for that run.

Final predictions of *in vivo* data are generated using a mixture of experts, where we train an ensemble of models with the same hyperparameters and average their predictions. Differences in weights generated during initialization, variations in the order in which data is fed to the algorithm during training, and the stochastic descent algorithm, introduces variation to the convergence of each model. Additionally, different validation sets were used in each run to avoid overfitting.

In vitro *training data: carbon fiber electrodes*

Data was collected from 76 of the same type of carbon fiber electrodes used in the DBS experiments.[19] For each electrode, generally four datasets were collected, one for each analyte (dopamine, serotonin, norepinephrine, and pH). The data acquisition equipment was of the same type (same component type/number) used in the *in vivo* data collection. Most of the three neuromodulators (dopamine, serotonin, and norepinephrine) datasets were collected with 30 concentrations of the analyte dispersed at equal intervals over the range from 0 to 2500 nM (nM), with a pH of around 7.4, while the other two analytes were kept at 0 nM. In addition, each of these datasets contained 5 mixture solutions for which the concentration of the neuromodulator in question was 840 or 1680 nM and one or two of the other neuromodulators had a concentration of 840 or 1680 nM. The fourth dataset for each electrode was collected with 11 pH values in the range 7.0–7.8 and with the concentration of the three neuromodulators set to 0 nM as well as 5 mixture solutions as described above. There are some electrodes with datasets that vary slightly in selection of the concentration vectors used within the ranges described above. Further, some electrodes have more than 4 datasets collected on them. The order of data collection within each neuromodulator set was randomized across concentrations and the order that each neuromodulator dataset was collected in was also randomized.

To collect data each electrode was deployed horizontally in a thin flow cell such that the carbon fiber and reference surfaces could be submerged in PBS. At the start of each dataset, the flow cell was filled with PBS and the electrode was pre-cycled at 97 Hz for approximately 10 min. We then filled the flow cell with varying concentrations of neuromodulators (as described above) and collected training data by running a 97 Hz pre-cycle protocol for 27 s followed by 65 s of our 10 Hz measurement protocol. We selected the most stable continuous 15 s section from the second half of the 10 Hz 65 s time window to reduce variation due to electrical noise and equilibration. Of these 76 electrodes, 6 were randomly held out to be used for model testing and the other 70 were used in the training process. The training set contained 2,594 unique concentration vector electrode combinations and 1,170,150 sweeps. The test set contained 803 unique concentration vector electrode combinations and 135,450 sweeps.

In vitro *model training: carbon fiber electrodes*

The data from the 70 training electrodes were pooled into a dataset with 150 current sweeps from each unique electrode-concentration combination. The model was a mixture of experts, where the final prediction is the average of an ensemble of 20 training runs. Current sweeps were always first-differenced prior to use in the training data. For each training run, the dataset was split into a training set containing around 90% of the data and a validation set containing the remainder. The data was split by electrode-concentration, such that all data points of any given concentration for a given electrode were in the same set. The data labels were z-scored within analyte. After training, the inverse of the normalization procedure was applied to model estimates obtained from new current inputs. The models were trained for 35 epochs.

In vitro *model evaluation: carbon fiber electrodes*

To evaluate the carbon fiber prediction models, neuromodulator (and pH) estimates were generated from the differentiated current traces from the 6 electrodes held out as the test set. The mean of the estimates from the 20-model ensemble was calculated. (see Figure 1B).

In vitro *training data: epilepsy electrodes*

Modeling data was collected from 6 explanted ACC electrodes that were used to collect *in vivo* participant data. For each electrode, generally four datasets were collected, one for each analyte (dopamine, serotonin, norepinephrine, and pH). The data acquisition equipment was of the same type (same component type/number) used in the *in vivo* data collection. Most of the three neuromodulators (dopamine, serotonin, and norepinephrine) datasets were collected with 30 concentrations of the analyte dispersed at equal intervals over the range from 0 to 2500 nM (nM), with a pH of around 7.4, while the other two analytes were kept at 0 nM. In addition, each of these datasets contained 5 mixture solutions for which the concentration of the neuromodulator in question was 840 or 1680 nM and one or two of the other neuromodulators had a concentration of 840 or 1680 nM. The fourth dataset for each electrode was collected with 11 pH values in the range 7.0–7.8 and with the concentration of the three neuromodulators set to 0 nM as well as 5 mixture solutions as described above. There are some electrodes with datasets that vary slightly in selection of the concentration vectors used within the ranges described above. The order of data collection within each neuromodulator set was randomized across concentrations and the order that each neuromodulator dataset was collected in was also randomized.

To collect data each electrode was dunked vertically into a 1.5 mL Eppendorf (containing the neuromodulator concentration of interest for that collection run) such that the working and reference microcontacts were submerged. We then collected current data at 10 Hz for 65 s using the same measurement protocol deployed during *in vivo* collection. We selected the most stable continuous 15 s section from the second half of the 10 Hz 65 s time window to reduce variation due to electrical noise and equilibration. See Bang et al., 2023 for previously published methods.

In vitro *model training: epilepsy electrodes*

Since the models on the depth electrodes data did not generalize across different electrodes, for each explanted electrode, a mixture of experts was trained, where the final prediction was the average of an ensemble of 5 training runs. A training run involved a dataset containing 150 sweeps from each unique concentration, that was split into a training set containing 90% of the data and a validation set containing the remainder. The data were split by concentration, such that all data points of any given concentration were in the same set. Before training, the data was z-scored within analyte, and then shifted by 10 standard deviations for each analyte to avoid zero gradients. After training, the predictions were then subjected to the inverse of the normalization procedure. The models were trained for 100 epochs.

In vitro *model evaluation: epilepsy electrodes*

A 10-fold cross-validation test was performed from explanted Ad-Tech depth electrodes. The *in vitro* data was split into 10 discrete folds without overlapping entries. Each fold was held out as a test set and an ensemble of models was created via a training run on the remaining data. Ensembles of four models were used instead of five to reduce computation time. The mean of the predictions from each 4-model ensemble was calculated for its corresponding test set. All test sets were combined, resulting in all *in vitro* data points being predicted from ensembles of models that had never been trained or validated on those data points (see Figure 4B).

In vivo *concentration estimates: all electrodes*

We generated *in vivo* concentration estimates using the same ensemble of the carbon fiber model or depth electrode models described above. *In vivo* current traces were differentiated as in the training and then evaluated by each model, where average predictions across this ensemble of models (mixture of experts) were used as the concentration estimates.

Rodent electrochemistry and optical stimulation

In vivo *data acquisition*

DAT-Cre mice (Figures S1C–S1F, $N = 7$; Figures S1H–S1K, $n = 4$, a subset of those mice used in Figures S1C–S1F) were injected with an AAV to drive Cre-recombinase-dependent expression of channelrhodopsin (ChR2, AAV-DIO-hChR2(H134R)-EYFP, Addgene viral prep # 26973-AAV9) in midbrain dopaminergic cells (from bregma, AP: −3.16mm, ML: ±1.02mm, DV: −4.5mm). An optic fiber (400μm, Doric) was positioned 75μM above the site of viral infusion to enable light delivery to activate this opsin. DBH-Cre mice (Figures S1M–S1P, $N = 3$) were injected with an AAV to drive Cre-recombinase-dependent expression of ChR2 (ChR2, AAV-DIO-hChR2(H134R)-EYFP, Addgene viral prep # 26973-AAV9) in noradrenergic locus coeruleus (LC) cells (from bregma, AP: −1.34mm, ML: ±0.3mm, DV: −2.1mm). An optic-fiber (200μm, Doric) was positioned 75μM above the site of viral infusion to enable light delivery to activate this opsin. SERT-Cre mice (Figures S1R–S1U, $N = 3$) were injected with an AAV to drive Cre-recombinase-dependent expression of ChrimsonR (AAV-EF1a-DIO-ChrimsonR-mRuby2- KV2.1- WPRE-SV40, Addgene viral prep # 124603-AAV9) in serotonergic dorsal raphe nucleus (DRN) cells (from bregma, AP: −4.5 mm, ML: 0.0 mm, DV: −2.8 mm). An optic-fiber (400μm, Doric) was positioned 75μM above the site of viral infusion to enable light delivery to activate this opsin. To measure evoked dopamine, norepinephrine, and serotonin release, mice were anesthetized using isoflurane (1–2%) using a SomnoSuite system (Kent Scientific; Torrington, CT) and placed in a stereotaxic frame (Kopf Instruments; Tujunga, CA). We then implanted carbon fiber electrodes into the dorsal striatum (DS) in DAT-Cre mice, the hippocampus in DBH-Cre mice, and the amygdala in SERT-Cre mice (dorsal striatum from bregma = AP: +0.8 mm, ML: ±1.45 mm, DV: −3.0 to −3.7 mm; hippocampus from bregma = AP: −1.3 mm, ML: ±1.12, DV: −1.6 to −2.1; amygdala from bregma = AP: −1.06 mm, ML: ±2.65 mm, DV: −4.5 to −5.1 mm), approximately 4–6 weeks after AAV infusion. We used the *same* electrochemical approach and the *same* carbon fiber model presented in Figure 1B to produce estimates of evoked dopamine, norepinephrine, and serotonin in response to optogenetic stimulation (470nM LED for ChR2, Thorlabs; 635nM laser for ChrimsonR, Shanghai Laser & Optics Century Co.; waveform: 15mW, 50 Hz, 10ms pulse width for all). Stimulation events were separated by ∼3 min, controlled via manual trigger on a waveform generator (AFG1062, Tekronix), and time-locked by a TTL. As a control for non-specific effects of optical stimulation, we inter-leaved trials using light delivery with the same waveform parameters; however, we used red-shifted light for ChR2 (617 nM LED,Thorlabs), or a blue-shifted light for ChrimsonR (462nM laser, Shanghai Laser & Optics Century Co.). An average of 3 stimulations from each mouse were used to generate all graphs.

QUANTIFICATION AND STATISTICAL ANALYSIS

Rodent neurochemical data analysis

All neurochemical predictions from rodents were first processed using MATLAB software (MathWorks; Natick, MA). For each mouse Cre-line, 3 active stimulations and 3 inactive null stimulations were used to determine mean trace responses and area under the curve (AUC) within mouse (for serotonin, 1 mouse only had 1 null stimulation). AUC was quantified using the trapezoidal method (dopamine, 4 s window post-onset of stimulation; norepinephrine, 14 s window post-onset of stimulation; serotonin, 14 s window post-onset of stimulation). We utilized the *lmer* function in R Studio (R version 4.4.0) to analyzed each neuromodulator AUC using linear mixed-effects models. To compare AUCs between the active stimulation and inactive null stimulation within each Cre-line, we predicted AUC with light type as a fixed effect with random effects across mice (Equation 1). The model is specified below using Wilkinson notation:

$$AUC_{DA|5HT|NE} \sim light\ type + (1|\ mice) \quad \text{(Equation 1)}$$

To compare AUCs of dopamine, norepinephrine, and serotonin between each mouse Cre-line, we predicted AUC with neuromodulator type as a fixed effect with the random effects across mice (Equation 2). The model is specified below using Wilkinson notation:

$$AUC \sim 1 + neuromodulator\ type + (1|\ mice) \quad \text{(Equation 2)}$$

For the power manipulation in the DAT-Cre mice, we predicted AUC with power as a fixed effect with random effects across mice (Equation 3). The model is specified below using Wilkinson notation:

$$AUC_{DA} \sim power + (1|\ mice) \quad \text{(Equation 3)}$$

Where necessary, we investigated the pairwise difference among neuromodulators using Tukey's Honestly Significant Difference (HSD) test. These summaries are illustrated in Figure S1.

Human behavioral data analysis

We used MATLAB (MathWorks, Natick, MA) to do all behavioral analysis. For these analyses, we only considered trials where a response was made, operating under the assumption that if a response was not made, the participants were not paying attention. We analyzed reaction times (Figure S2) using linear mixed effects-models in MATLAB using the *fitglme* function where we predicted reaction times given word valence and arousal continuous ratings as a fixed effects with random intercept effects across participants (Equation 4). We ran the *anova* function over the model parameters and if any statistical significance

occurred we reported these F-values and *p*-values. We ran models with random effects across slopes and intercepts; the intercept models always had the lowest AIC. However, both models produced similar results. The model is specified below using Wilkinson notation:

$$Reaction\ Time \sim 1 + word\ valence + word\ arousal\ (1 \mid participant) \quad \text{(Equation 4)}$$

We also summarized the number of trials that had responses and the accuracy over word valence– these were similar across word valence (Figure S2).

Human neurochemical data analysis

General data handling

All neurochemical predictions from humans were analyzed using MATLAB software (MathWorks; Natick, MA). For these analyses, we only considered trials where a response was made, operating under the assumption that if a response was not made, the participants were not paying attention. Neurochemical data, aligned to word onset, for dopamine, serotonin, and norepinephrine were first smoothed by a 0.5 s window per trial across a 6-s snippet of data centered on word presentation. The mean and standard deviation were then calculated for each trial per neuromodulator across the same 6-s snippet of data centered on word presentation (i.e., representing 3 s before and 3 s after a given word was shown). The trials were then z-scored per neuromodulator on a trial-by-trial basis. Thus, each trial (each time a word was shown) was standardized to itself– we have performed similar processing in previous publications (e.g., Bang et al., 2020) and have found it to be useful in highlighting signal changes. The data were then broken into negative, positive, and neutral word valence. To calculate the max change measure, we took the 0.5 s mean before word onset and subtracted this from the rest of the time series on a trial-by-trial basis to create a time series that represented the change from pre-word baseline. We then ran an algorithm to find the largest change (positive or negative) during the time the word was on the screen (0–1.3 s). Note that we also experimented with AUC and whole time-series descriptions of the neuromodulator dynamics and the max change tended to capture the most consistent and clear trends in the time series; thus, we used max change for all of our linear mixed-effects analyses. We used the *fitglme* function to fit all linear mixed-effects models. We ran models with random effects across slopes and intercepts; the intercept models always had the lowest AIC. However, both models produced similar results. We ran the *anova* function over the model parameters and if any statistical significance occurred we reported these F-values and *p*-values. We interrogated any main effects or interactions using more specific linear mixed-effects models (see below). For all graphical representations, the data were broken into word valence, each neuromodulator was averaged separately per person (to create a mean per neuromodulator per word valence per person), then the mean and standard error were calculated over people and graphed.

Statistical modeling for VIM DBS participants

For our VIM measurements from DBS participants we performed linear mixed-effects analyses by creating an omnibus design matrix where each row was a trial and there was a column for the participants (coded numerically in an ordinal fashion, i.e., 1, 2, 3, etc.), word valence (using the numerical ANEW word ratings), word arousal (using the numerical ANEW word ratings), and reaction time (z-scored in order to control for variability in reaction time between operating room participants). We predicted neuromodulator max change using word valence, word arousal, and reaction time, as well as reaction time interactions, as fixed effects with the random effects across participants (Equation 5). The model is specified below using Wilkinson notation:

$$Max\ Change_{DA|5HT|NE} \sim 1 + (word\ valence + word\ arousal) * reaction\ time + (1 \mid participant) \quad \text{(Equation 5)}$$

Categorical modeling for VIM DBS participants

For our VIM measurements from DBS participants we performed categorical linear mixed-effects analyses, on the findings with significant results, by creating a design matrix where each row was a trial and there was a column for the participants (coded numerically in an ordinal fashion, i.e., 1, 2, 3, etc.), word valence (here using the categorical label), word arousal (here using the categorical label), and reaction time (z-scored in order to control for variability in reaction time between operating room participants). For these analyses, we used the categorical labels for valence, focusing only on negative and positive (negative = −1; positive = 1), and arousal (arousing = 1; neutral = −1) to increase rigor and to make direct comparisons between groups (oppose to just as a function of valence or arousal).

In the random word task, we only observed a significant main effect of arousal for norepinephrine using our omnibus continuous linear mixed-effects model so we followed that up with a categorical model where we predicted norepinephrine max change using categorical word arousal, reaction time, as well as their interactions, as fixed effects with the random effects across participants (Equation 6). The model is specified below using Wilkinson notation:

$$Max\ Change_{NE} \sim 1 + word\ arousal * reaction\ time + (1 \mid participant) \quad \text{(Equation 6)}$$

In the blocked word task, we only observed a significant main effect of valence for serotonin using our omnibus continuous linear mixed-effects model so we followed that up with a categorical model where we predicted serotonin max change using categorical

word valence, reaction time, as well as their interactions, as fixed effects with the random effects across participants (Equation 7). The model is specified below using Wilkinson notation:

$$Max\ Change_{5HT} \sim 1 + word\ valence_{Neg\ vs\ Pos} * reaction\ time + (1 \mid participant) \quad \text{(Equation 7)}$$

Considering we observed significant valence effects with serotonin in the blocked design, we also wanted to see if there were differences across dopamine and serotonin within valence. Thus, we utilized a linear mixed-effects categorical model where we predicted the max change of dopamine and serotonin for negative or positive words given neuromodulator type (dopamine = 1 and serotonin = 2), reaction time (z-scored), and their interactions (Equation 8). The model is specified below using Wilkinson notation:

$$Max\ Change_{Neg|Pos} \sim 1 + neuromodulator\ type_{DA|5HT} * reaction\ time + (1 \mid participant) \quad \text{(Equation 8)}$$

Statistical modeling for ACC epilepsy participants

For our ACC measurements from epilepsy participants we performed linear mixed-effects analyses by creating an omnibus design matrix where each row was a trial and there was a column for the participants (coded numerically in an ordinal fashion, i.e., 1, 2, 3, etc.), word valence (using the numerical ANEW word ratings), word arousal (using the numerical ANEW word ratings), reaction time (z-scored in order to control for variability in reaction time between participants), and hemisphere (modeled categorically; 0 = left, 1 = right). We predicted neuromodulator max change using word valence, word arousal, reaction time, and hemisphere, as well as reaction time and hemisphere interactions with word valence and arousal, as fixed effects with the random effects across participants (Model 9). The model is specified below using Wilkinson notation:

$$Max\ Change_{DA|5HT|NE} \sim 1 + (word\ valence + word\ arousal) * reaction\ time * hemisphere + (1 \mid participant) \quad \text{(Equation 9)}$$

Categorical modeling for ACC epilepsy participants

For our ACC measurements from epilepsy participants we performed categorical linear mixed-effects analyses, where results were significant, by creating a design matrix where each row was a trial and there was a column for the participants (coded numerically in an ordinal fashion, i.e., 1, 2, 3, etc.), word valence (here using the categorical label), word arousal (here using the categorical label), reaction time (z-scored in order to control for variability in reaction time between participants), and hemisphere (modeled categorically; 0 = left, 1 = right). For these analyses, we used the categorical labels for valence, focusing only on negative and positive (negative = −1; positive = 1), and arousal (arousing = 1; neutral = −1) to increase rigor and to make direct comparisons groups (oppose to just as a function of valence).

We first found a significant valence x reaction time interaction for serotonin in the ACC. To probe this interaction, we first looked at the effect of hemisphere, reaction time, and their interactions on the max change of serotonin for negative and positive valence individually (Equation 10). The model is specified below using Wilkinson notation:

$$Max\ Change_{5HT\ Neg|5HT\ Pos} \sim 1 + reaction\ time * hemisphere + (1 \mid participant) \quad \text{(Equation 10)}$$

We also wanted to probe the effect of valence across reaction times. To do this, we binned the reaction time data into fast (all data below the lower quartile per participant) and slow (all data above the upper quartile per participant) and assessed the effect of valence, hemisphere, and their interactions on the max change of serotonin within fast and slow reaction times (Equation 11). The model is specified below using Wilkinson notation:

$$Max\ Change_{5HT\ Fast|5HT\ Slow} \sim 1 + word\ valence_{Neg\ \&\ Pos} * hemisphere + (1 \mid participant) \quad \text{(Equation 11)}$$

In the ACC the omnibus model revealed a valence × hemisphere interaction for dopamine. We probed this interaction by using a categorical linear mixed-effects model with valence, reaction time, and their interactions to assess dopamine levels within a single hemisphere (each hemisphere was modeled separately) across valence (Equation 12). The model is specified below using Wilkinson notation:

$$Max\ Change_{DA\ Right|DA\ Left} \sim 1 + word\ valence_{Neg\ \&\ Pos} * reaction\ time + (1 \mid participant) \quad \text{(Equation 12)}$$

We also wanted to assess changes within valence (modeled separately) across hemisphere. To do this, we ran a categorical linear mixed-effects model that included hemisphere, reaction time, and their interactions to assess dopamine levels (Equation 13). The model is specified below using Wilkinson notation:

$$Max\ Change_{DA\ Neg|DA\ Pos} \sim 1 + hemisphere * reaction\ time + (1 \mid participant) \quad \text{(Equation 13)}$$

In the ACC the omnibus model revealed a trend level arousal × hemisphere interaction for norepinephrine. We probed this interaction by using a categorical linear mixed-effects model with arousal, reaction time, and their interactions to assess the max change of norepinephrine within a single hemisphere (each hemisphere was modeled separately) across valence (Equation 14). The model is specified below using Wilkinson notation:

$$Max\ Change_{NE\ Right|NE\ Left} \sim 1 + word\ arousal * reaction\ time + (1 \mid participant) \quad \text{(Equation 14)}$$

We also wanted to assess changes within arousal (modeled separately) across hemisphere. To do this, we ran a categorical linear mixed-effects model that included hemisphere, reaction time, and their interactions to assess the max change in norepinephrine (Equation 15). The model is specified below using Wilkinson notation:

$$Max\ Change_{DA\ Neutral|DA\ Arousing} \sim 1 + hemisphere * reaction\ time + (1 \mid participant) \quad \text{(Equation 15)}$$